PIPERAZINE FUNCTIONALIZED MAGNETIC SPOROPOLLENIN FOR SOLID PHASE EXTRACTION OF LEAD(II)

NAQHIYAH FARHAN BINTI AHMAD

FACULTY OF SCIENCE
UNIVERSITY OF MALAYA
KUALA LUMPUR

2018

PIPERAZINE FUNCTIONALIZED MAGNETIC SPOROPOLLENIN FOR SOLID PHASE EXTRACTION OF LEAD(II)

NAQHIYAH FARHAN BINTI AHMAD

THESIS SUBMITTED IN FULFILMENT OF THE REQUIREMENTS FOR THE DEGREE OF MASTER OF SCIENCE

DEPARTMENT OF CHEMISTRY
FACULTY OF SCIENCE
UNIVERSITY OF MALAYA
KUALA LUMPUR

2018

UNIVERSITY OF MALAYA

ORIGINAL LITERARY WORK DECLARATION

Name of Candidate: Naqhiyah Farhan binti Ahmad

Matric No: SGR 150009

Name of Degree: Master of Science

Piperazine functionalized magnetic sporopollenin for solid phase extraction of lead(II)

Field of Study: Analytical Chemistry

I do solemnly and sincerely declare that:

(1) I am the sole author/writer of this Work;
(2) This Work is original;
(3) Any use of any work in which copyright exists was done by way of fair dealing and for permitted purposes and any excerpt or extract from, or reference to or reproduction of any copyright work has been disclosed expressly and sufficiently and the title of the Work and its authorship have been acknowledged in this Work;
(4) I do not have any actual knowledge nor do I ought reasonably to know that the making of this work constitutes an infringement of any copyright work;
(5) I hereby assign all and every rights in the copyright to this Work to the University of Malaya ("UM"), who henceforth shall be owner of the copyright in this Work and that any reproduction or use in any form or by any means whatsoever is prohibited without the written consent of UM having been first had and obtained;
(6) I am fully aware that if in the course of making this Work I have infringed any copyright whether intentionally or otherwise, I may be subject to legal action or any other action as may be determined by UM.

Candidate's Signature Date:

Subscribed and solemnly declared before,

Witness's Signature Date:

Name:

Designation:

PIPERAZINE FUNCTIONALIZED MAGNETIC SPOROPOLLENIN FOR SOLID PHASE EXTRACTION OF LEAD(II)

ABSTRACT

The present work describes the successful functionalization/magnetization of bio-polymeric spores of *Lycopodium Clavatum* (sporopollenin) with 1-(2-hydroxyethyl) piperazine. Characterization techniques i.e., Fourier Transform Infra-red (FT-IR), Field Emission Scanning Electron Microscope (FESEM), Energy-Dispersive X-ray Spectroscopy (EDS), Powder X-Ray Diffraction (PXRD) and Vibrating Sample Magnetometer (VSM) were used to confirm the formation of 1-(2-hydroxyethyl) piperazine functionalized magnetic sporopollenin (MNPs-Sp-HEP**)**. The proposed material was used as an adsorbent for the adsorption of noxious Pb(II) ions metal ion from aqueous media through a batch-wise method. Adsorption isotherm studies revealed that Langmuir model well-fitted to experimental data as compared to Freundlich isotherm. Maximum adsorption capacity (q_m) of Pb(II) ions is 13.29 mg g^{-1}. Thermodynamic parameters such as free energy (ΔG°), entropy (ΔS°) and enthalpy (ΔH°) were also investigated from the adsorption studies and were used to elaborate the mechanism of their confiscation. The successful synthesized modified sporopollenin was future optimized for magnetic solid-phase extraction (MSPE) of Pb(II) ions from environmental samples. The pre-concentration and determination of Pb(II) ions were conducted by Flame Atomic Absorption Spectroscopy (FAAS). The best working conditions were as follow; pH 6.5, 15 min of extraction time, 0.3 mol L^{-1} HNO_3 as elution solvent, 10 min of desorption time and 25 mg of adsorbent dosage. Under the optimized condition, the analytical performances were determined with pre-concentration factor (PF) and limits of detection (LOD) are 47 and 0.005 mg L^{-1}, respectively. The reusability studies suggested that the newly synthesized adsorbent

could be used up to five cycles. The proposed method was performed to analyze Pb(II) ions in real water samples from river water, tap water and leachates.

Keywords: Sporopollenin, Piperazine, Magnetic Solid Phase Extraction, lead(II) ions

PEMFUNGSIAN MAGNETIK SPOROPOLLENIN OLEH PIPARAZIN UNTUK PENGEKSTRAKAN FASA SOLID LEAD(II)

ABSTRAK

Kajian ini menerangkan kejayaan pemfungsian/pemagnetan spora biopolymer daripada Lycopodium Clavatum (Sporopollenin) dengan 1-(2-hidroksiletil) piparazin yang telah berjaya. Teknik pencirian seperti Inframerah Transformasi Fourier (FT-IR), Mikroskopi Elektron Pengimbas Pancaran Medan (FESEM), Spektroskopi Tenaga Serakan Sinar-X (EDX), Spektroskopi Pembelauan Sinar-X (PXRD) dan Magnetometer Sampel Bergetar (VSM) digunakan untuk mengesahkan pembentukan 1-(2-hidroksiletil) piparazin yang difungsikan dengan sporopollenin bermagnet (MNPs-Sp-HEP). Bahan yang dicadangkan digunakan sebagai bahan penjerap untuk menjerap ion logam Pb(II) ion yang berbahaya dari media akueus melalui kaedah "batch-wise". Kajian penjerapan isoterma mendedahkan bahawa model Langmuir bersesuaian dengan data eksperimen berbanding model Freundlich. Kapasiti penjerapan maksimum ion Pb(II) ion adalah 13.29 mg g^{-1}. Parameter termodinamik seperti tenaga bebas ($\Delta G°$), entropi ($\Delta S°$) dan entalpi ($\Delta H°$) telah dikaji daripada kajian penjerapan dan telah digunakan untuk menghuraikan mekanisma antara penjerap dan ion Pb(II) ion. Sporopollenin yang diubahsuai telah berjaya disintesis seterusnya dioptimumkan untuk pengekstrakan fasa pepejal magnetik (MSPE) bagi ion Pb(II) ion daripada sampel alam sekitar. Pra- kepekatan dan penentuan Pb(II) ion telah dijalankan oleh Spektroskopi Penyerapan Atom Nyalaan (FAAS). Keadaan terbaik pengekstrakan adalah seperti berikut; pH 6.5, 15 minit sebagai masa pengekstrakan, 0.3 mol L^{-1} HNO_3 sebagai pelarut, 10 minit bagi masa nyahjerapan dan 25 mg bagi dos penjerap. Di bawah keadaan optimum, prestasi analisis telah ditentukan oleh faktor pra kepekatan (PF) dan had pengesanan ialah 47 dan 0.005 mg L^{-1}. Kajian guna semula mencadangkan bahan

penjerap yang baru disintesis boleh diguna semula sehingga lima kali penggunaan. Kaedah yang dibangunkan digunakan untuk menganalisis ion Pb(II) ion di dalam sampel air dari sungai, air paip dan air larut serapan.

Kata kunci: Sporopollenin, Piparazin, Pengekstrakan bermaknetik fasa solid, ion plumbum(II)

ACKNOWLEDGEMENTS

Thanks to Allah S.W.T The Mighty and The Creator of the world, by this blessing and kindly, thus I can complete my research project by the time given. Firstly, I would like to express my gratitude to my supervisor Assoc. Prof. Dr. Sharifah Mohamad for her capable guidance, valuable advice, untiring patience and invaluable support that she has provided during the years that I spent at University Malaya (UM). I am grateful for her technical supervision, helpful discussion, and the cooperation, versatility and enthusiasm she has exemplified in allowing me to pursue my research.

My acknowledgement and thousands of thanks also goes to Dr Siti Nadiah Abd Halim as my co-supervisor who always support me even she was busy on her work. Thanks for giving me the guidance and willing to share the experiences during my research.

I cannot express in words how grateful I am to my parents, Ahmad bin Desa and Manih binti Muhammad Saad for their unconditional love, patience and blessings. I would to thank my brother and sisters for constant encouragement and unwavering support during the study. Not to forget my fiancé, Mohd Afiq who support me days and nights. To these special peoples I am eternally grateful.

My gratitude also goes out to Dr Afzal and Dr Hamid who contributed to my understanding and comprehension of the research and modelling study greatly. Also special thanks to University Malaya for giving me grant PG049-2015B for me to complete the study.

Lastly, in this opportunity, I would like to thank especially to Siti Khalijah, Nurul Yani, Fairuz Liyana, Siti Farhana, Nur Faizah, Aisha, labmate of FD-L5-4 and my housemates because of their willingness to spend their time in helping me to complete

this project and also for their full support and encouragement in this research project. Thanks for always being there for me. All of you will be missed.

TABLE OF CONTENTS

LIST OF FIGURES

LIST OF TABLES

LIST OF SYMBOLS AND ABBREVIATIONS

$\Delta G°$	:	Free energy
$\Delta H°$	:	Enthalpy
$\Delta S°$	:	Entropy
b	:	Langmuir adsorption constant
C_e	:	Equilibrium ion concentration
k_1	:	First order rate constant
k_2	:	Second order rate constant
K_F	:	Freundlich adsorption capacity
k_{id}	:	Intraparticle diffusion rate constant
n	:	Freundlich adsorption intensity
q_e	:	Amounts of Pb(II) ions (mg g^{-1}) absorbed at equilibrium
q_m	:	Maximum adsorption capacity
q_o	:	Maximum surface density at monolayer coverage
q_t	:	Amounts of Pb(II) ions (mg g^{-1}) absorbed at time,
R^2	:	Correlations coefficient
γ-MPTMS	:	γ-mercaptopropyltrimethoxysilane
CAC	:	*p-tert*-butylcalix[4]-aza-crown
CPTS	:	3-cyanopropyltrimethoxysilane
CPTS-Sp	:	*3*-cyanopropyltriethoxysilane modified Sporopollenin
EDL	:	Electrodeless discharge lamp
EDS	:	Energy-Dispersive X-ray Spectroscopy
FAAS	:	Flame Atomic Absorption Spectroscopy
Fe_3O_4	:	Iron Oxide
FESEM	:	Field Emission Scanning Electron Microscope

FT-IR	:	Fourier Transform Infra-red
GA	:	Glutaraldehyde
H_2SO_4	:	Sulphuric acid
HCl	:	Hydrochloric acid
HEP	:	1-(2-Hydroxyethyl) piperazine
HNO_3	:	Nitric acid
HPBA	:	(E)-4-((2-hydroxyphenylimino) methyl) benzoic acid
HSAB	:	Pearson acid base concept
ICP	:	Inductively Coupled Plasma
LLE	:	Liquid-liquid extraction
LOD	:	Limit of detection
LOQ	:	Limit of quantifications
MNPs	:	Magnetic nanoparticles
MSPE	:	Magnetic Solid-Phase Extraction
Pb(II)	:	Lead(II)
PF	:	Preconcenration factor
PXRD	:	Power X-Ray Diffraction
RSDs	:	Relative standard deviations
SCMNPs	:	Silica-coated magnetic nanoparticles
Sp	:	Sporopollenin
SPE	:	Solid phase extraction
Sp-HEP	:	Sporopollenin functionalized with 1-(2-hydroxyethyl) piperazine
VSM	:	Vibrating Sample Magnetometer
WHO	:	World Health Organization

CHAPTER 1: INTRODUCTION

1.1 Background of Study

Recently industrial sectors discharge a huge amount of effluents which contain variety of highly toxic as well as persistent pollutants such as dyes, phenols, pesticides and heavy metals (Liu *et al*., 2010; Sáez *et al*., 2014; He 2015; Meenakumari and Philip 2015; Vymazal and Brezinova 2015; Bakhshaei *et al*., 2016; Shahabuddin *et al*., 2016). The release of the untreated effluents to the natural stream is of great anxiety because due to rapidly growing urbanization and industrialization the scale of contaminated effluents is escalating day by day.

Industrial units like mining, smelting, battery manufacturing and recycling activities are renowned for the Pb(II) ions contamination (Cheng *et al*., 2015; He 2015). In some countries, the usage of leaded paint and leaded aviation fuel has contributed to lead contamination in our environment (Gulson *et al*., 2016; Wolfe *et al*., 2016). Despite that, products for instant pigments, paints, solder, stained glass, crystal vessels, ammunition, ceramic glaze, jewelry, toys and in some cosmetics and traditional medicines also contributed to the excess of lead ion in the environment (Selwyn, 2005).

Lead species (tetraethyl lead) was first introduced as an anti-knocking agent in petrol in 1922 to improve the effectiveness of fuel and to decrease wear on vehicle engines (Landrigan, 2002). By 1970s, almost all petrol produced around the world contained lead. However, the disadvantages of lead in petrol are more crucial than its benefits. The toxic effect of lead had cause public health become worst when exposed to lead worldwide and cause more environmental lead exposure than any other sources. Therefore, in the year 1994 the United Nation commissions called on governments worldwide including Malaysia to change from leaded to unleaded petrol (Singh and Singh, 2006).

In Malaysia, most of the manufacturing industries that contribute to lead contamination are located on the west coast of Peninsular Malaysia. In Malacca Strait, port and shipping activities contribute to Pb(II) ions ion pollution (Ibrahim and Khalid, 2007). The concentration of Pb(II) ions indicates some enhancement above the natural global value (in shale) in the coast of Kemaman, Tanjung Karang and off Juru, Penang (Farid *et al*., 2016). The high value of Pb(II) ions in the Johor Strait between Malaysia and Singapore was maybe due to the use of leaded petrol (Shazili *et al*., 2006).

The extensively used of Pb(II) ions has caused bad environmental contaminations and thus, the human exposure has resulted in significant public health problems around the world (Kabata-Pendias, 2011).

The toxicity of Pb(II) ions has had serious consequences for the health especially for young children (Rauh and Margolis 2016). They may suffer profound health effects at the higher level of Pb(II) ions exposure such as mental retardation and behavioral disorders. At low level of exposure, lead can reduce the children intelligent quotient (IQ) which will decrease the educational attainment. On the other hand, lead can increase the risk of high blood pressure and kidney damage in adults. The exposure of high levels of lead to pregnant women can cause miscarriage, stillbirth, premature birth and low weight, as well as minor malformations (WHO, 2016).

In this regard, the world health organization (WHO) has set maximum residual level 0.01 mg L^{-1} in water samples. Meanwhile, Ministry of Health Malaysia has fixed a Drinking Water Quality Standard which is 0.05 mg L^{-1} and 0.01 mg L^{-1} for recommended raw water quality and drinking water quality standard respectively. The Ministry of Domestic Trade, Co-operative and Consumerism (MDTCC) regulated mandatory safety standards for toys intended for children below 14 years old. Under the MS ISO 8124-3 Safety of Toys Part 3 Migration of Certain Elements, the maximum

acceptable migration of lead in paint shall not be more than 90 mg L^{-1}. Thus, precise monitoring, determination, and remediation of noxious Pb(II) ions metal ions from the environment are extremely important for human health.

However, it is a challenge to determine Pb(II) ions in the environmental sample as it exists in a trace amount and the intervention of a complex matrix. Therefore, a new technique for separation and/or pre-concentration step before analysis is very important. Solid-phase extraction (SPE) technique is known as such kind of sample pretreatment method and it has become more and more popular due to its high enrichment factor, simple operation, and minimal cost, reusability of the adsorbent and easy automation.

Different types of materials have been used for SPE approaches such as activated carbon, silica base materials, polymers and biomass (Aguado *et al*., 2009; Ucar *et al*., 2014; Jain *et al*., 2015; Lapwanit *et al.*, 2016). For SPE process, the structure of adsorbent plays an important role in order to enhance mechanical, chemical and thermal stability. Bio-polymeric spores of Lycopodium Clavatum (sporopollenin), possesses tremendous mechanical, thermal and chemical stability. Additionally, sporopollenin can be easily functionalized/magnetized due to the high content of functional groups (Paunov *et al*., 2007). Numerous modifications on the surface of sporopollenin have been done by various researchers (Çimen *et al*., 2014; Kamboh *et al*., 2016; Şener *et al*., 2016).

To obtain selective adsorption of Pb(II) ions, amine functionalized adsorbents are considered as eminent and was previously reported (Georgiou *et al*., 2016; Nonkumwong *et al*., 2016). According to Pearson acid base concept (HSAB), this functional group shows higher selectivity toward Pb(II) ions. In addition, iron oxide nanoparticles are capable to reduce the time consumed for the determination of the analyte and also can be easily separated from aqueous solution (Wan Ibrahim *et al.,*

2016). The specific characteristics of iron oxide nanoparticles provide a convenient tool for exploring magnetic separation techniques (Hola *et al*., 2015). The higher surface area offered by magnetic particles has improved the adsorption behaviour compared to that of the raw biosorbent (Sureshkumar and Daniel, 2016). Magnetically modified biosorbent reveals promising adsorption capacity toward mixed wastewaters (Sivashankar *et al*., 2014).

In this research, sporopollenin was modified with 3-cyanopropyltrimethoxysilane (CPTS) and functionalized with 1-(2-hydroxyethyl) piperazine (Sp-HEP). The functionalized sporopollenin was magnetized with iron oxide nanoparticles (MNPs-Sp-HEP). The combination of amine ligand and iron oxide nanoparticles with sporopollenin enhanced the adsorption properties of sporopollenin and resulting in strong binding affinities toward Pb(II). The synthesized of MNPs-Sp-HEP was used to investigate its performance as an adsorbent for the extraction of Pb(II). Thus, in order to investigate the adsorption properties of this new adsorbent, isotherm, kinetic and thermodynamic studies have been investigated. In addition, new MSPE method has been developed and validated for the extraction of Pb(II) ions from environmental samples.

1.2 Objective of Study

The aim of this study is to develop new piperazine functionalized magnetic sporopollenin (MNPs-Sp-HEP) as an adsorbent for the extraction of Pb(II) ions from environmental water samples prior to Flame Atomic Absorption Spectroscopy (FAAS) analysis. The objectives of this study are as follows:

a) To synthesis and characterize piperazine functionalized magnetic sporopollenin (MNPs-Sp-HEP),

b) To evaluate the adsorption behavior of Pb(II) ions using MNPs-Sp-HEP,

c) To develop and validate MSPE method for the extraction of Pb(II) ions from aqueous solution using MNPs-Sp-HEP and

d) To apply MNPs-Sp-HEP for the extraction of Pb(II) ions from environmental samples.

1.3 Thesis Outline

The present thesis is organized into five chapters. Chapter 1 gives a brief introduction on background and research objectives. A review of related literature is presented in Chapter 2. Chapter 3 covered experimental methodologies on the preparation and functionalization of sporopollenin (Sp) embedded magnetic nanoparticles (MNPs), screening studies, adsorption studies of Pb(II) ions with MNPs-Sp-HEP and application of MNPs-Sp-HEP as a sorbent for MSPE of Pb(II) ions. Chapter 4 presented results and discussion which divided into three parts. First part is the characterization of synthesized materials. Meanwhile, in the second part, the result of adsorption studies of Pb(II) ions with MNPs-Sp-HEP was elaborated, whereas last part discussed on the application of MNPs coated sporopollenin-piperazine as a sorbent for MSPE of Pb(II) ions and real sample analyses. Finally, the overall conclusions, together with the recommendation of future works are provided in Chapter 5.

CHAPTER 2: LITERATURE REVIEW

2.1 Heavy Metals

Metals, such as zinc, functions as a cofactor for several enzymatic reactions in the human body. Cobalt and iron, on the other hand, function as a component in vitamin B-12 and hemoglobin, respectively. These metals are essential to human biochemical processes (Bridwell-Rabb and Drennan, 2017). Similarly, cobalt, selenium, manganese, iodine, iron, zinc and molybdenum are trace elements that are important to the human diet (Nielson, 1990). Other metals are extensively used for therapeutic medicine, such as aluminium, bismuth, gold, gallium, lithium, and silver, all of which are a part of the medical armamentarium (Thompson and Orvig, 2003). These elements are dangerous if taken in large quantities or in the event that the usual mechanisms of elimination are impaired. However, many other metal elements that are considered heavy metals have no known benefit for human physiology, with lead, mercury and cadmium being prime examples of such "toxic metals".

Heavy metals are toxic at low level exposures due to its relatively higher density than water (Jaishankar *et al*., 2014). They are also considered as trace elements due to their trace presence in the (ppb range, to less than 10 ppm) in various environmental matrices (Kabata-Pendias and Pendias, 2001). Although heavy metals are naturally occurring elements found throughout the Earth's crust and natural activities (Tchounwou *et al*., 2012), most heavy metal pollution in the environment are the result of anthropogenic activities, such as mining and smelting operations, industrial production and use, and domestic and agricultural use of metals and non-metal containing compounds (He *et al*., 2005; Begum and Huq 2016). Natural phenomena, such as weathering and volcanic eruptions, have also been reported to significantly contribute to heavy metal pollution (He *et al*., 2005; Wang *et al*., 2009).

The toxicity of heavy metals depends on a number of factors, such as the total dose absorbed, age of the person, and acute/chronic weather exposure (Adal and Tarabar, 2014).

2.1.1 Pb(II) ions

Lead is a heavy metal that carries an atomic number of 82, atomic weight of 207.19, and a specific gravity of 11.34. It is a bluish-grey metal in its natural state, and is only present in small amounts in the Earth's crust. Pb(II) ions exists in many forms in its natural state throughout the world, and is now one of the most widely and evenly distributed trace metals. It can also contaminate soils and plants and can harm biological systems due to the fact that it does not undergo biodegradation (Tangahu *et al*., 2011).

Pb(II) ions is not naturally present in the human body. It is currently exists in the environment, and is classified as a health hazard. It is a versatile metal that has been used since the prehistoric era. It has become widely distributed and mobilized in the environment, which accounts for its exposure to humans in the form of its increased uptake. High levels of lead exposure damage all organs and organ systems, especially the central nervous system, kidneys, and blood, which could culminate in death (Kader *et al*., 2016).

2.1.1.1 Sources of Pb(II) ions in Environment

Occupations, such as mining, manufacturing, and construction will inevitably result in Pb(II) ions exposure. The US Centres for Disease Control and Prevention (CDC) defines an elevated blood level of Pb(II) ions in adults to be above 25 μg/dL. In 2007, 6463 (76.7%) of elevated blood levels were found to be the result of occupational exposure, while in 2011, there were 2151 reported cases of Pb(II) ions exposure. Of these exposures, 1023 were reported to be in children younger than 5 years old, and 643 in those older than 20.

Lead is a soft metal that reports variety of applications over the years in cables, and pipeline, paints, and pesticides. Due to its widespread applications, Pb(II) ions can enter the food chain via multiple routes. For example, plants uptake Pb(II) ions from the soil and the air, which results in Pb(II) ions being deposited on their respective surfaces. Fishes could be exposed to Pb(II) ions from water and sediments, while other mammals could be exposed to Pb(II) ions via the food they consumed.

Anthropogenic activities, such as fossil fuels burning, mining, and manufacturing contribute to increasing amounts of Pb(II) ions in the ecosystem. Pb(II) ions has many different industrial, agricultural, and domestic applications. It is currently used in the production of lead-acid batteries, bullets, metal products (solder and pipes), and devices to shield X-rays (Sears *et al*., 2012). ~1.52 million metric tons of lead were used for various kinds of industrial applications in the United States in 2004, and of that amount, lead acid batteries production accounted for the majority (83%), while the remaining usage encompass a variety of products, such as ammunitions (3.5%), oxides for paint, glass, pigments, and chemicals (2.6%), and sheet lead (1.7%) (Tchounwou *et al*., 2012).

Recently, the use of lead in industries has reported a decrease from paints and ceramic products, caulking, and pipe solder. Despite this fact, it has been reported that among 16.4 million US homes with more than one child younger than 6 years, 25% of them still report significant amounts of lead-contaminated paint, dust, or adjacent bare soil (Jacobs *et al*., 2002). The dust and chips from deteriorating lead paint on interior surfaces often re-contaminates clean houses, contributing to high blood lead concentrations in children.

There are various industries that contribute to lead contamination in South and Southeast Asian countries, such as Peninsular Malaysia, Vietnam, India, Thailand, Philippines, Indonesia, Bangladesh, and Pakistan, (Clark *et al*., 2006). In Malaysia, the

paint industry is fast becoming one of the industries that contributes to lead contamination of Malaysian waters, according to the Consumer Association of Penang (CAP).

Paint contains high levels of lead when the paint manufacturer intentionally adds one or more leaded compounds to the paint. Exposure could also take place when paint ingredients are contaminated with Pb(II) ions, or cross-contaminated by other product lines within the same factory. Solvent based enamel paints have been found to have high lead content in many countries; however, water-based paints rarely report contamination with lead (Brosché *et al*., 2014; Clark *et al*., 2006; Clark *et al*., 2009).

A previous study conducted by the Consumers' Association of Penang (CAP) in 1992 found that seven out of nine enamel paints (78%) contained lead above 600 parts per million (ppm). The highest reported amount of lead in that study was 11,700 ppm. An earlier study analysed paints purchased between 2004 – 2007, and found that fifty percent of the paints contained lead above 600 ppm, while 31 percent of paints contained lead levels above 10,000 ppm.

In September 2015, the Consumers' Association of Penang (CAP) purchased 39 cans of solvent based enamel decorative paint from stores in the states of Penang and Kedah in Malaysia. The samples were analysed by a laboratory in the US for their total lead content based on the dry weight of the paint. Sixteen out of 39 enamel decorative paints (41% of paints) reported a total lead concentration exceeding 600 ppm. Moreover, 12 samples (31%) contained significantly high concentration of lead, at >10,000 ppm. The highest lead concentration detected was 150, 000 ppm, whilst the lowest was less than 60 ppm.

In Malaysia, there is currently no regulation in place limiting the amount of lead in paint for household and decorative uses. However, the Ministry of Domestic Trade, Co-operatives and Consumerism (MDTCC) regulated mandatory safety standards for toys intended for children below 14 years old. Under the MS ISO 8124-3 Safety of Toys PART 3 Migration of Certain Elements, the maximum acceptable migration of lead in paint cannot be more than 90 ppm.

2.1.1.2 Toxicity of Pb(II) ions Towards Human Health

In the environment, Pb(II) ions is particularly noxious to plants, animals, and microorganism due to its high level of toxicity. The effects of Pb(II) ions toxicity are generally limited to contaminated areas. Pb(II) ions contamination in environment poses serious human health problems and risks, namely, brain damage and retardation (Tangahu *et al*., 2011).

Early exposure of Pb(II) ions could harm children and fetuses, as they predispose them to a lifetime of lifetime of multisystem ailments, as well as lower IQ and dysfunctional behavior. For people who are older, there is the risk of increased of early health decline, as well as suffering from a range of conditions, including kidney and cardiovascular disease, diabetes, and osteoporosis (Sears *et al.*, 2012).

Studies showed that Pb(II) ions has no essential function in humans; it can only harm after being uptaken from the air or water. Pb(II) ions can result in several unwanted effects, such as brain damage, mental deficiency, anemia and behavioral problem if inhaled (Gupta and Rastogi, 2008) It is recommended that the amount of Pb(II) ions be measured in various cities to allow for these cities to implement preventive action that could reduce the adverse effect of Pb(II) ions on the environment and people. A separation and/or pre- concentration step is always required prior to analyses of Pb(II) ions due to its amount in trace level and matrix effect.

2.2 Solid Phase Extraction (SPE)

Solid-phase extraction (SPE) is one of the techniques that can be used to pre-treat samples. The high enrichment factor, simple operation, minimal cost, reusability of the adsorbent, and easy automation offered by SPE accounts for its favoured status among researchers.

SPE was first introduced in the mid-1970s (Liška, 2000). Initially, this technique was established to complement of completely replace liquid-liquid extraction (LLE) (Mohamad, 2014). This is because many problems caused by LLE, such as incomplete phase extraction, use expensive and breakable specialty glassware, less than quantitative recoveries and wastage of large quantities of organic solvent can be prevented. SPE is simple, and report high pre- concentration factor, rapid phase separation, the ability to combine via multiple detection techniques and decreased usage of organic solvents which directly benefits the environment (Aboul- Enein, 2003).

The principle of SPE is similar to that of LLE. Both involve partitioning solutes between two phases. However, SPE partitions a liquid (sample matrix or solvent with analytes) and a solid (sorbent) phase, while LLE involves two immiscible liquid phases. This technique allows the concentration and purification of analytes from solution via sorption on a solid sorbent and purification of extracts post-extraction.

The interaction between the sorbent and analytes of interest will affect the selection of an appropriate sorbent for SPE extraction. It is therefore dependent on the knowledge of the hydrophobic, polar, and inorganic properties of both the solute and sorbent. The most common retention mechanisms in SPE are based on van der Waals forces (non-polar interaction), hydrogen bonding, dipole-dipole forces (polar interaction), and cation – anion interactions (ionic interaction). A variety of extraction problems can be solved, as each sorbent offer a unique combination of these properties.

The main format in SPE is the syringe-barrel and cartridge types. The SPE cartridge is a small plastic or glass open ended container filled with adsorptive particles of various types and adsorption characteristics. The cartridge type is still the most popular format, with typically 40-60 µm dp packing material. Limitations of packed SPE conventional cartridges include restricted flow-rates and plugging of the top frit when handling water-containing suspended, solid such as surface water or waste water (Moldoveanu and David, 2015). Currently, a large number of sorbents are used as sorbent for SPE of heavy metals, such as ion exchanger resin (Rossi *et al*., 2017).

However, the quick separation of the adsorbent from the solution and decreasing the separation time are still complexities of the method that needs to be solved. The features of magnetic adsorbent that can subsided rapidly under a magnetic field is effective for magnetic separation (Rozi *et al*., 2017). Therefore, combined SPE and magnetic nanoparticles will form magnetic solid phase extraction (MSPE), which is suitable for pre- concentration and separation studies.

2.2.1 Magnetic Solid Phase Extraction (MSPE)

In 1909, Gunther reported a powerful separation approach (magnetic separation technology) in complex industrial, bio-separation, and environmental and material science based on the use of magnetic or magnetisable adsorbent (Tripathy *et al*., 2017). This new SPE type based on the use of magnetic or magnetizable adsorbent has attracted much interest in separation science (Vasconcelos and Fernandes, 2017).

Magnetic nanoparticles (MNPs) have been used as adsorbent in extraction due to their high surface area, small particle sizes, ease of dispersion in water, and modification viability to increase its surface area and adsorption capacity. It was first introduced in 1999 by Safarikova and Safarik. The magnetic nanoparticles adsorbent

does not need to be packed into an SPE cartridge, it can be dispersed in a sample solution (Gao *et al*., 2010).

Additionally, MSPE can be used to directly analyse the samples, because particles or microorganisms are abundant in the environment (Aguilar-Arteaga *et al.,*2010). MNPs should be subjected to proper surface modification prior to MSPE. Figure 2.1 shows the schematic procedure of MSPE for pre-concentration and separation from aqueous media.

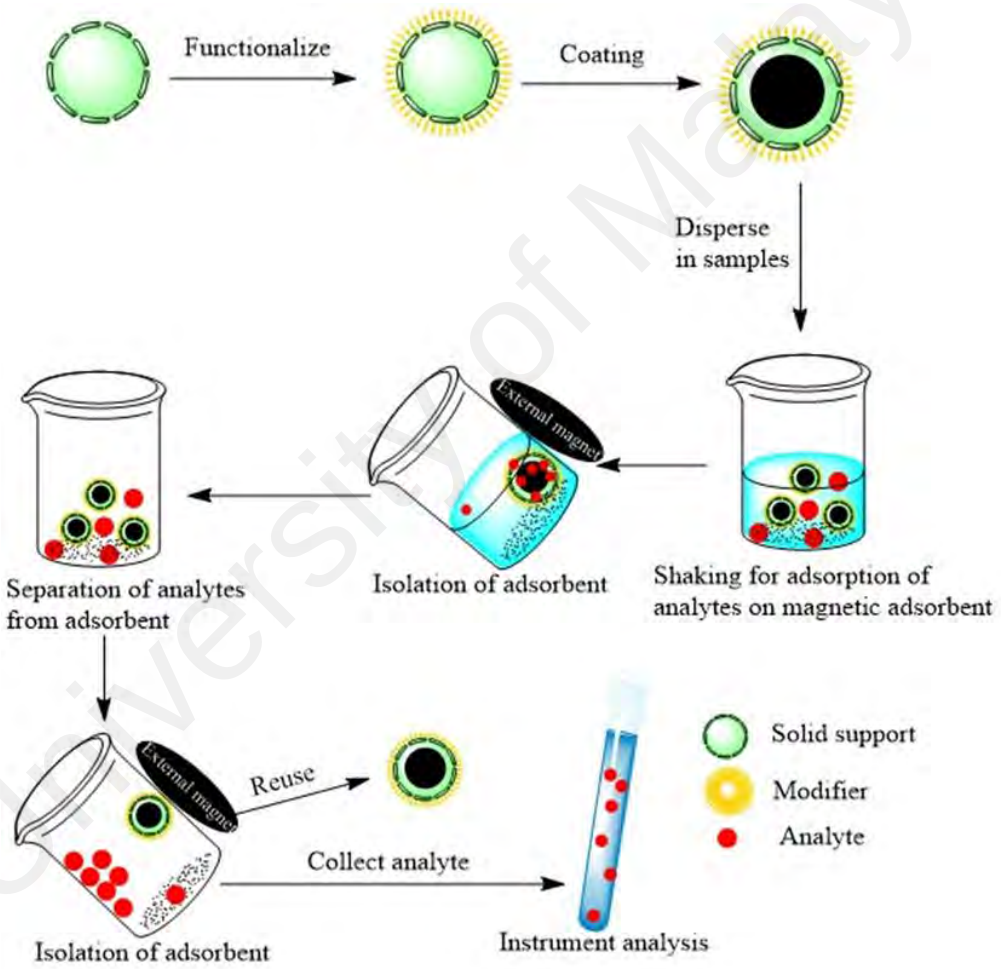

Figure 2.1 Illustration for the application of magnetic nanoparticles in magnetic solid-phase extraction (MSPE) (Wan Ibrahim et al., 2015)

2.2.2 Iron oxide nanoparticles: Adsorbent in MSPE

Nanoparticles can be made from inorganic/organic materials. These submicron moieties report many novel properties compared to bulk materials. Nanoparticles encompass a wide range of disciplines, namely magnetic fluids, data storage, separation, catalysis, and bioapplications due to its unique magnetic properties, such as superparamagnetic, high coercivity, low Curie temperature, and high magnetic susceptibility (Wu *et al*., 2008). Nanoparticles are unique because it can be tailored to specific applications due to high surface area-to-volume ratio, which provides surface functionalization.

Magnetic nanoparticles include iron oxides, ferrites of cobalt, manganese, nickel, magnesium, and platinum. However, iron oxide is the only nanomaterial that has been permitted for use by the US Food and Drug Administration (US FDA), as it is considered biological safe (Ali *et al*., 2016).

Superparamagnetic nanoparticles (NPs), mostly based on iron oxides magnetite (Fe_3O_4), hematite (α-Fe_2O_3), or maghemite (γ-Fe_2O_3), are increasingly being studied in the past decade due to its potential for multiple applications in pharmacology as both therapeutic and diagnostic agents, including their use in targeted drug delivery systems allowing for manipulation by external magnetic field, as contrast agents for magnetic resonance imaging or for cancer treatment by magnetic heating therapy (Wozniak *et al*., 2017).

Known as black iron oxide, magnetite reports the sturdiest magnetism amongst transition metal oxide. Hematite, typically known as ferric oxide or martite, is abundant in rocks and soils. They are blood-red in colour in bulk, and grey in coarse crystal. Maghemite can be formed from heating of iron oxides or weathering (Majewski and Thierry, 2007).

High surface area, superparamagnetism, simple preparation step, the provision for surface modification, being inert, biocompatibility, low toxicity, and low cost are some of the advantages offered by magnetic nanoparticles in the context of waste water treatment (Boyer *et al*., 2010; Gupta and Gupta, 2005; Pan *et al*., 2010).

The capability of iron oxide nanoparticles to extract pollutants has been proven both experimentally and in actual environmental settings (Girginova *et al*., 2010; White *et al*., 2009). The process has been combined with adsorptive process for water and environmental purification, especially as a solid sorbent in a magnetic solid-phase extraction (MSPE) (Ambashta and Sillanpaa, 2010; Mahdavian and Mirrahimi, 2010).

However, the small size of iron oxide nanoparticles resulted in distinct disadvantages. It gets unstable due to its higher surface energy, and tends to agglomerate in solutions to reduce its surface energy (Lin *et al*., 2005). Its stability affects the electrostatic and Van der Waals interactions between the nanoparticles (Chen *et al*., 2007). Bare metallic nanoparticles are chemically active and readily oxidizes, which could reduce its magnetism and ability to disperse (Xie *et al*., 2014). Thus, the surface of magnetite has been chemically functionalized to overcome the stability problem using appropriate groups (Boyer *et al*., 2010; Dias *et al*., 2011). Modification strategy include grafting and coating the surface of magnetite. Furthermore, the functionalization/modification could also result in functional properties that can be tailored for bespoke applications.

2.2.3 Application of MSPE for the extraction of Pb(II) ions from aqueous sample.

A magnetic nano-adsorbent, coated with titanium dioxide and polypyrrole (PPys) (Fe_3O_4/ TiO_4/ PPy), was successfully used for magnetic solid-phase extraction and pre-concentration of trace amounts of Pb(II) ions as a simple and effective absorbent. Under

optimal conditions, the limit of detection and maximum adsorption capacity were reported to be 0.28 μg L^{-1} and 126 mg g^{-1}, respectively. The accuracy of the method was determined by analyzing its Certified Reference Material (CRM), with the reported value being in excellent agreement with the CRM. The method was simple, quick, and sensitive, making it applicable for analysing trace/ ultra-trace Pb(II) ions in complex matrices (Mehdinia *et al*., 2017).

The detection of ultra-trace amounts of Pb(II) ions in biological samples using ICP-MS was realised after the separation and pre-concentration with a functionalized Fe_3O_4/GO nanocomposite with an aptamer. The successfully functionalized biosorbent can effectively and repeatedly be used to detect Pb(II) ions from blood and urine samples. Its advantage includes the economic consumption of functional aptamer as an affinity probe. Using a suitable aptamer in separation and pre-concentration process is an excellent alternative to classical ligands. Moreover, the method is simple, highly selective, reports low detection limits, is highly efficient, and report high enrichment factor (Shamsipur *et al*., 2017).

Iron oxide magnetic nanoparticles (Fe_3O_4-NPs) were synthesized using the co-precipitating method under optimised condition by Sadeghi and his co-workers. The Fe_3O_4 -NPs, coated with sodium dodecyl sulfate-thenoyltrifluoroacetone (Fe_3O_4-NPs-SDS-TTFA), were then exerted as a magnetic solid phase extraction (MSPE) adsorbent to extract Pb(II) ions from water samples prior to introducing it to a flame atomic adsorption spectrometry (FAAS). The high surface area of nanoparticles and rapid magnetic separation led to an excellent detection limit and enrichment factor of 2.3 μg L^{-1} and 250, respectively. The method is also simple and sensitive enough for the analysis of large volumes of sample solution (Sadeghi *et al*., 2016).

A novel magnetic ion-imprinted polymer (Fe_3O_4@SiO_2@IIP) was synthesized using 3-(2-aminoethylamino) propyltrimethoxysilane (AAPTS) as its functional monomer, tetraethylorthosilicate (TEOS) as its cross-linker, and Pb(II) ions as its template, and evaluated for the selective extraction of Pb(II) ions from environmental samples via the magnetic solid phase extraction (MSPE) procedure. The obtained Fe_3O_4@SiO_2@IIP was well dispersed, reporting an average size of 200 nm. This magnetic imprinted adsorbent exhibited excellent selectivity towards Pb(II) ions, with a selectivity factor of over 3.75 in the presence of Cu(II), Zn(II), Cd(II), and Hg(II). When a magnetic absorbent was used in MSPE, excellent recoveries (>98.0%) for Pb(II) ions were reported in environmental samples under optimized conditions. The magnetic imprinted adsorbent can be applied for the rapid extraction of Pb(II) ions from environmental samples (Zhang *et al*., 2011).

2.3 Sporopollenin (Lycopodium Clavatum)

Plant spores from the species Lycopodium clavatum have long been used as a natural powder lubricant, a base for cosmetics, and as herbal medicine. This is mostly due to its availability, low cost, and chemical robustness. It can be found in fossil green algae, moss, ferns, liverwort, bryophytes, and even fungi.

According to Brooks and Shaw (1978), sporopollenin (Sp) has been described as the most resistant organic materials of direct biological origin found in nature and in geological samples. Sp is a common club moss that can be found in many areas and rocky slopes in Europe, Central and South America, and Asia and Africa. Sp has been used as a cheap flammable powder for pyrotechnics since the 19th century, and has also been largely used as a drying and dusting agent, both in folk medicine and modern pharmaceuticals (Orhan *et al*., 2007).

Sp, which is the biopolymer shell of pollen grains of higher plants, is a highly resilient yet poorly characterised material. It has been defined as "one of the most extraordinary resistant materials known in the organic world" (Paunov and Stoyanov 2007). The exact chemical nature of Sp remains obscure, and it is fairly reliant on the development stage and source, due to differences in the degrees of polymerisation, saturation or cross-linking, or the proportion and order of its monomers. Since differences are apparent from species to species, the word "sporopollenin" actually refers to a family of natural polymeric compounds that noticeably prevail in pollen and spores exines (Brooks and Shaw 1972; Mackenzie *et al*., 2016). Field Emision Scanning Electron Microscope (FESEM) images show that the structure of Sp consist of Laesura, Murus, and Lumen (Figure 2.2).

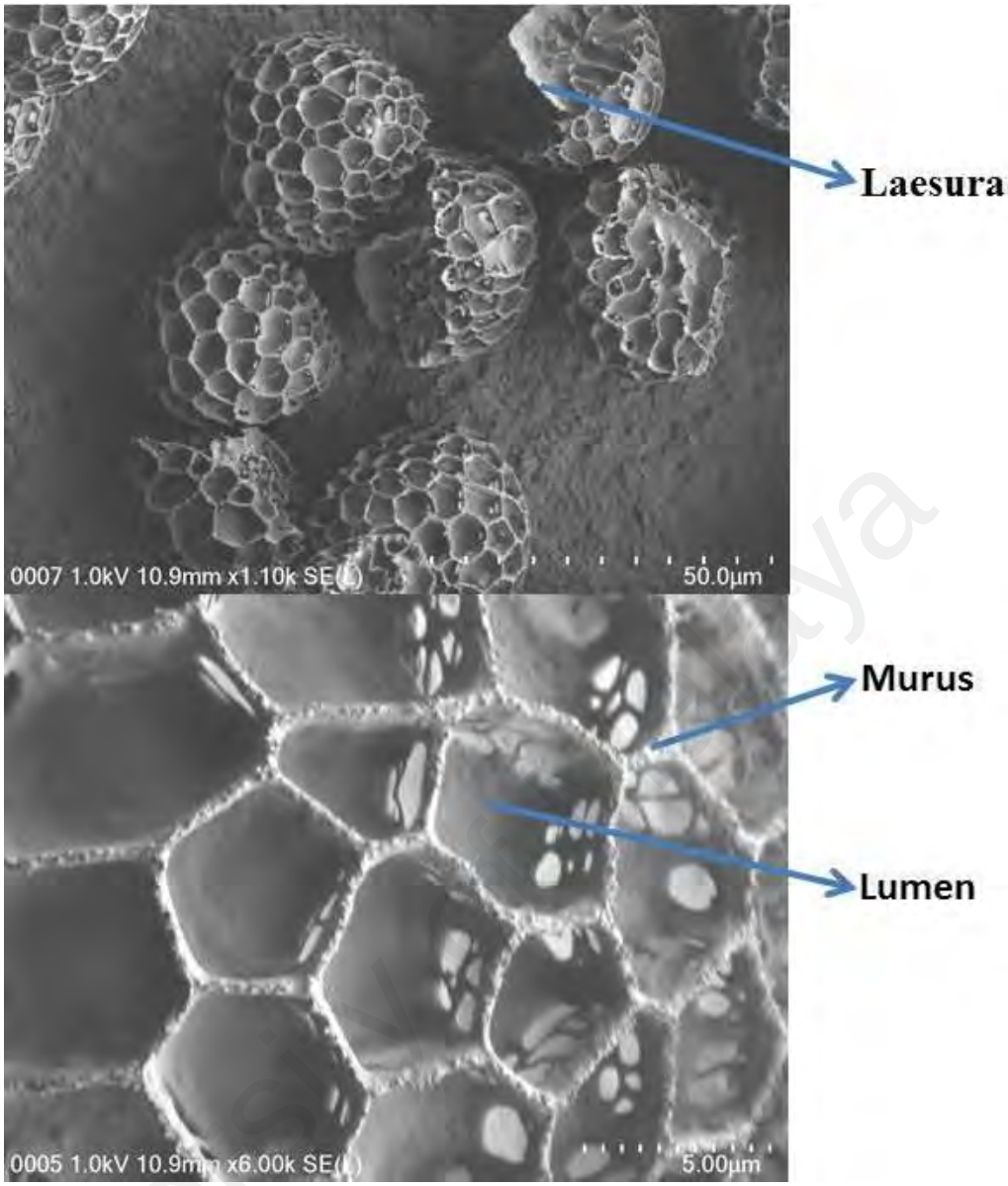

Figure 2.2 Lycopodium Clavatum spores

2.3.1 Properties of Sporopollenin

Sporopollenin, as shown in Figure 2.3, is a natural polymer obtained from Lycopodium clavatum, which is highly stable and resistant to chemical attacks. It is extremely tough, resistant to acid and alkali degradation, and has been shown to pass unchanged though the digestive system of animals. Sp has an aromatic character that contains carbon, hydrogen, and oxygen, with a stoichiometry of $C_{90}H_{44}O_{27}$ (Gubbuk *et*

al., 2012). Analyses showed that the Sp is a mixture of biopolymers containing mainly long chain fatty acids, phenylpropanoids, phenolics, and traces of carotenoids.

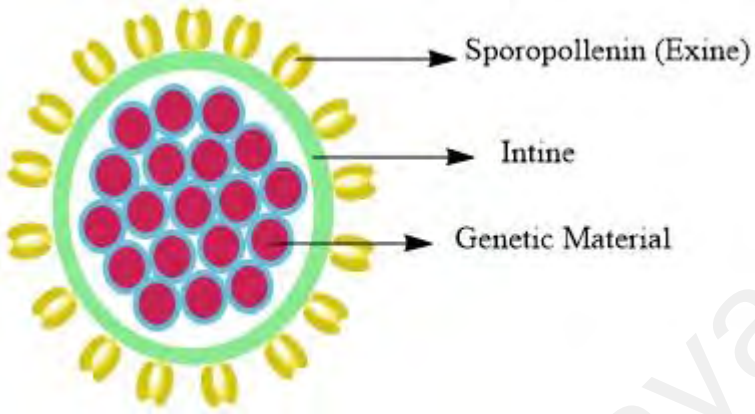

Figure 2.3 Schematic diagram of spore/ pollen particle

Sporopollenin particles are also remarkably resistant against physical, biological, and chemical non-oxidative aggressions (Diego-Taboada *et al*., 2014). The refractive index of sporopollenin (Kettley, 2001) and its specific gravity confirms the compact nature of the material itself. This makes it largely insoluble in most common solvents (Brooks and Shaw, 1972).

Spores float on water and are barely wetted. This can be explained by the presence of fat (pollenkitt and/ or tryphine) coatings on spores. It can also be explained by the fact that the chemical structure of sporopollenin is very hydrophobic due to its hydrocarbon skeleton. On the other hand, empty exines only float for a set amount of time, but seems to progressively absorb water, which prompts it to eventually sink. Contrarily, sporopollenin readily soak up oils and organic solvents, especially ethanol, and they very quickly produce a suspension due to them being highly monodispersed.

Sporopollenin is a complex framework of mainly cross-linked saturated aliphatic chains, with some of it being unsaturated. Attached to its chains are oxygenated functional groups, including carboxylic acids, lactones, hydroxyls, and phenols (Toriyama, 2011).

The chemical structure of Sp is a controversial issue. There are few features of Sp that have been established; (i) Sp is composed of carbon, hydrogen, and oxygen, with a C/H ratio 5/8 (mol/mol), such as terpenes. Sp is constituted of an aliphatic matrix that is common to most species of vascular plants (ferns, gymnosperms and angiosperms), and (ii) the carbon skeleton is cross-linked by various side-groups whose exact nature, position, and number are directly species-dependent.

2.3.2 Modified Sporopollenin and its Application in Extraction of Metals

The modification of Sp was achieved by chemically immobilizing suitable organic groups onto its surface. In this process, organic reagents are directly attached to support surfaces.

(E)-4-((2-hydroxyphenylimino) methyl) benzoic acid (HPBA) immobilized sporopollenin was employed as an adsorbent to absorb heavy metal ions in aqueous solutions. The sorbent material was prepared by sequential treatment of sporopollenin with salinising compound and HPBA. The result calculated from adsorption isotherm model and thermodynamics indicates that this sorbent was successfully employed to separate trace Cu(II), Ni(II), and Co(II) from aqueous solutions (Çimen *et al*., 2014).

Sporopollenin was modified with solid support and used as an adsorbent to remove contaminated effluents. The adsorbent was prepared using functionalized Fe_3O_4 nanoparticles with calix(4)arene, and conjugated with N-methylglucamine. It showed a significant percent sorption (84%) of boron in aqueous environment (Kamboh and Yilmaz, 2013).

p-tert-butylcalix[4]-aza-crown (CAC) immobilized Sp was used as a sorbent to remove Cu(II), Pb(II), and Zn(II) from aqueous media. It was prepared by functionalising Sp with 3-chloropropyltrimethoxysilane (CPTS), followed by CAC. The

results show that the factors governing the sorption characteristics of immobilized sorbent competed for the H^+ ions with the metal ion at low pH value, at a maximum sorption at pH 5.0 – 5.5, and at higher pH levels precipitation of hydroxyl species onto the sorbent being more predominant (Gubbuk *et al.,* 2012).

Glutaraldehyde (GA) immobilized sporopollenin (Sp) is employed as a sorbent to absorb selected heavy metal ions. It was prepared by sequential treatment of Sp by silanasing compound and glutaraldehyde for the sorption of Cu(II), Zn(II) and Co(II) from aqueous solutions. Chemical modification of Sp was attempted with glutaraldehyde using the immobilisation method to yield the chelating material Sp-APTS-GA. Metal sorption followed the order of $Co^{2+} > Zn^{2+} > Cu^{2+}$ for the removal of metal ion. The Sp-APTS-GA material reported a high adsorption capacity for all metal ions. It can be concluded that the sorbent system is practical and efficient for the removal of heavy metals contaminants from synthetic and industrial effluents, owing to its low cost, ready availability, and environmental friendliness (Gubbuk, 2011).

CHAPTER 3: METHODOLOGY

3.1 Chemical and reagents

All chemicals used were analytical grade; ultra-pure water was used throughout this work. The chemicals and solvent were used as received and without further purification. 1-(2-Hydroxyethyl) piperazine (HEP), 3-cyanopropyltriethoxysilane (CPTS) and sporopollenin (Sp) were purchased from Sigma-Aldrich (Steinheim, Germany). Ferric chloride hexahydrate ($FeCl_3.6H_2O$), ferrous chloride tetrahydrate ($FeCl_2.4H_2O$), 30% ammonia solution and toluene were from R&M Chemicals (Malaysia). Working standard solutions were prepared daily by diluting the stock standard solution with deionizing water to the required concentrations.

3.2 Instrumentation

Fourier transform infrared spectroscopy (FT-IR) measurements were recorded on a Perkin Elmer RX1 FT-IR spectrometer (Massachusetts, USA) with the sample prepared as KBr pellets. All spectra were run in the range of 400- 4000 cm^{-1} at room temperature. Powder X-ray diffraction (PXRD) measurements were performed on a PAN analytical EMPYREN (Panalytical, Almelo, Netherlands) with monochromated Cu K α radiation (λ=15.4187 A) over the angular range from 15° to 75° (2θ) and with a scan speed of 0.07°/min and a step size of 0.026°. The size and morphology of resulting product were investigated using a HITACHI SU8220 Field Emission Scanning Electron Microscope (FESEM) (Hillsboro, USA). Energy Dispersive X-Ray analysis (EDX) which is attached to FESEM instrument is used to identify the elemental analysis of the product. The magnetic property was tested using a vibration sample magnetometer (VSM) Model 9600 (Quantum Design Inc., San Diego, USA). An ultrasonicator (Power Sonic 405, South Korea) was used for dispersion all the solutions in this study. For pH adjustment, HI 2213 pH/ORP Meter (HANNA instrument, Rhode Island, US) was used. A flame atomic absorption spectrometer (FAAS) Perkin Elmer Analyst 400 (Uerlingen,

Germany) equipped with an electrodeless discharge lamp (EDL) for lead was used in the analyses. The FAAS was operated with acetylene and airflow rates of 2.5 L min^{-1} and 10.0 L min^{-1} respectively.

3.3 Synthesis method of MNPs-Sp-HEP

Herein, the functionalization, as well as magnetization of 3-cyanopropyltriethoxysilane modified Sporopollenin (CPTS-Sp**)** with 1-(2-hydroxyethyl) piperazine (HEP) and Fe_3O_4 respectively, in order to obtain a new MNPs-Sp-HEP (Figure 3.1) is reported for the first time.

3.3.1 Modification of sporopollenin with 3-Cyanopropyltriethoxysilane (CPTS)

Sporopollenin functionalized with 3-Cyanopropyltriethoxysilane (CPTS) was prepared according to the previously reported method (Çimen et al. 2014). 10 g sporopollenin was suspended in 67 mL dry toluene and 6 mL of CPTS was added. The mixture was then refluxed for 72 hours and dried under vacuum (Figure 3.1(i)). The percentage yield obtained is 69%.

3.3.2 Functionalization of 3-Cyanopropyltriethoxysilane (CPTS) modified sporopollenin (Sp) with 1-(2-hydroxyethyl) piperazine (HEP)

10 g of freshly prepared Sp-CPTS was treated with 25% (v/v) of 1-(2-hydroxyethyl) piperazine (HEP**)** solution and stirred at room temperature for 15 h (Figure 3.1 (ii)). After the filtration of the suspension, the residue was washed with deionized water. The Sp-HEP was then dried under vacuum at 80 °C for 20 hours. The percentage yield is 76%.

3.3.2 Magnetization of Sp-HEP (MNPs-Sp-HEP)

13.32 g of $FeCl_3.6H_2O$, 19.88 g of $FeCl_2.4H_2O$, 5 mL 5 mol L^{-1} HCl, 40 mL ultrapure distilled water and 5 mL ethanol were mixed in a 100 mL flask. The solution

was heated to 40 °C until complete dissolution of the salts. Then, 1 g Sp-HEP was redispersed in 30 mL of this solution and stirred for 2 h at room temperature. The Sp-HEP suspension was filtered and quickly washed with ultrapure distilled water on the filter and then immediately transfered into 1 mol L^{-1} ammonia solution. After 2 h stirring at room temperature, the magnetic sporopollenin functionalized HEP (Figure 3.1 (iii)) was collected by an external magnet and washed thoroughly with ultrapure distilled water and dried under vacuum at 80 °C for 20 hr (Kamboh and Yilmaz 2013). The percentage yield of MNPs-Sp-HEP is 71%.

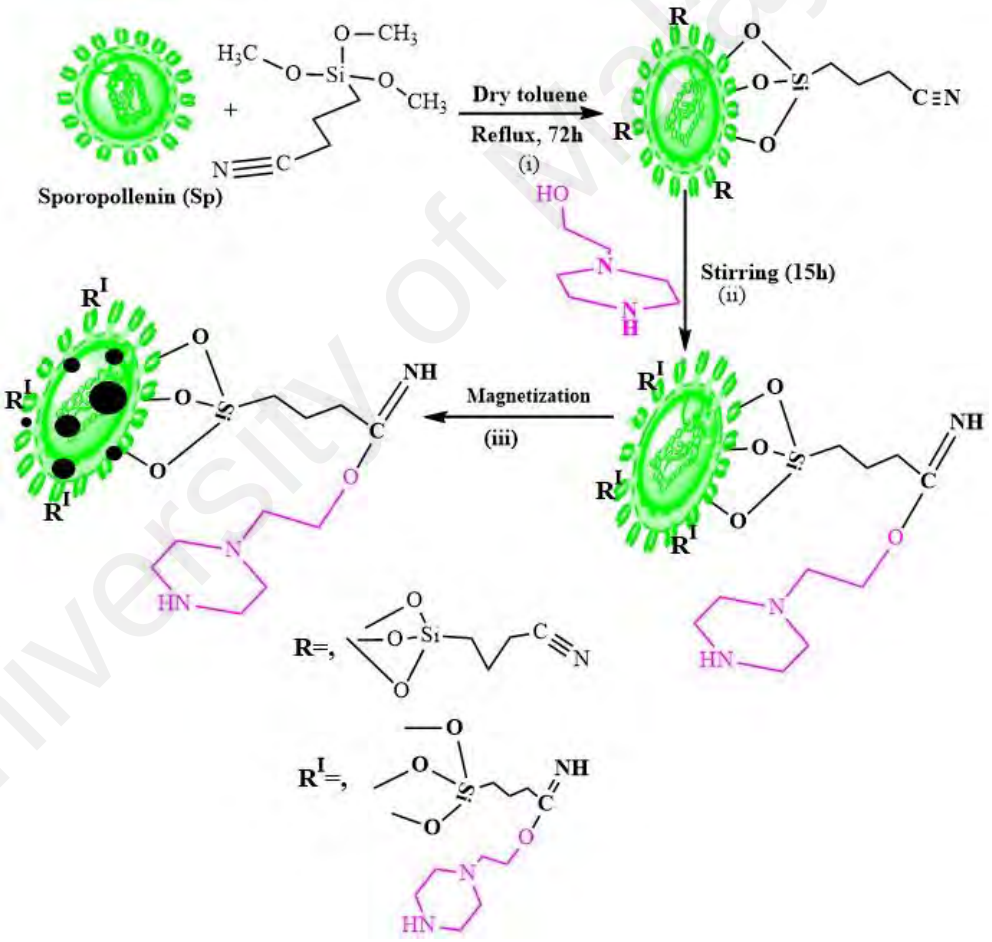

Figure 3.1 Schematic routes for the preparation of MNPs-Sp-HEP. (i) Preparation of Sp-CPTS (ii) Preparation of Sp-HEP (iii).Magnetization of Sp-HEP.

3.4 Characterization

All the samples were characterized using FTIR, FESEM, EDX, XRD, and VSM techniques.

3.5 Screening Study

The potential of MNPs, sporopollenin, and MNPs-Sp-HEP as an adsorbent have been investigated in this section. Experiment data were determined by the following procedure: In each experiment 10 mg of the sorbent was placed in 50 mL centrifuge tube, 10 mL of Pb(II) ions solution (10 μg L^{-1}) was added to the tube. Then, the mixture was shaken mechanically for 30 minutes at 25°C, and the adsorbent was removed using an external permanent magnet. The residual concentration of Pb(II) ions was determined using FAAS.

3.6 Adsorption Study

The adsorption of Pb(II) ions from water was performed by using batch equilibrium method. Figure 3.2 shows the schematic procedure of the batch adsorption study. Initially, the adsorbent dosage studied was from 10 mg to 50 mg and the solution pH was from 3.5 to 6.5 with 5-25 min adsorption time. After each adsorption treatment, an external magnet was applied for magnetic adsorbent separation from the solution. The residual concentration of Pb(II) ions in the water samples was measured using FAAS.

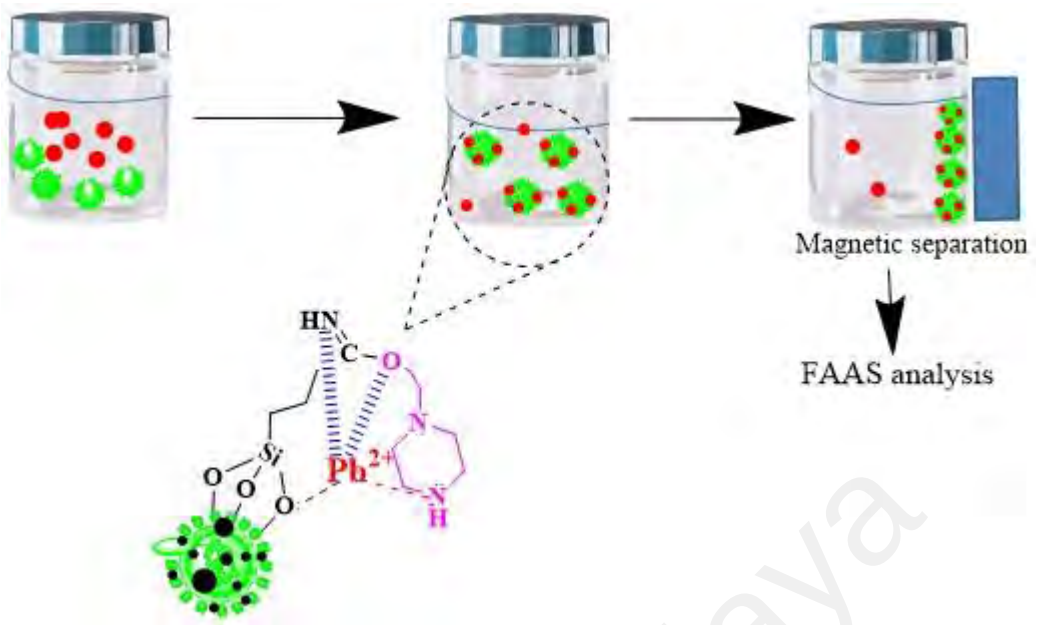

Figure 3.2 Schematic procedures for adsorption of Pb(II) ions by using MNPs-Sp- HEP. (Optimum conditions: Dosage of MNPs-Sp-HEP = 25 mg, sample pH = 6.5, time = 15 minutes)

3.7 Procedure for MSPE

140 mL of sample solution of 10 µg L^{-1} of Pb(II) ions was placed into 500 mL plastic bottle, and the solution pH was adjusted to pH 6.5 with an appropriate amount of 0.1 mol L^{-1} HCl. Then, 25 mg of adsorbent was added to the solution to reach sorption equilibrium. The beaker was shaken mechanically for 15 minutes at room temperature, and the adsorbent was removed using an external permanent magnet. The solution was decanted, and the external magnet was removed from the tube wall, leaving the MNPs in the tube. Then, 3 mL of HNO_3 (desorption solvent) at concentration 0.3 mol L^{-1} was added, and the mixture was sonicated for another 10 minutes. Finally, magnetic adsorbent was collected via an external magnet, and the desorbed analyte solution was analyzed using FAAS for Pb(II) ions determination. The MSPE process and FAAS determination were performed in triplicate.

3.7.1 Optimization of MSPE Process

Factors affecting the extraction efficiency of the proposed method such as pH, extraction time, sample volume, elution solvent volume, desorption time, and adsorbent dosage were studied. The study and optimization of the above-mentioned variables were performed using one variable at a time method (Figure 3.3). The final concentration of Pb(II) ions was used to evaluate the influence of the factors on the extraction efficiency of MSPE of the Pb(II) ions. All the experiments were performed in triplicate and reusability studied was conducted for seven cycles to determine the possibilities for reutilizing and regeneration were investigated.

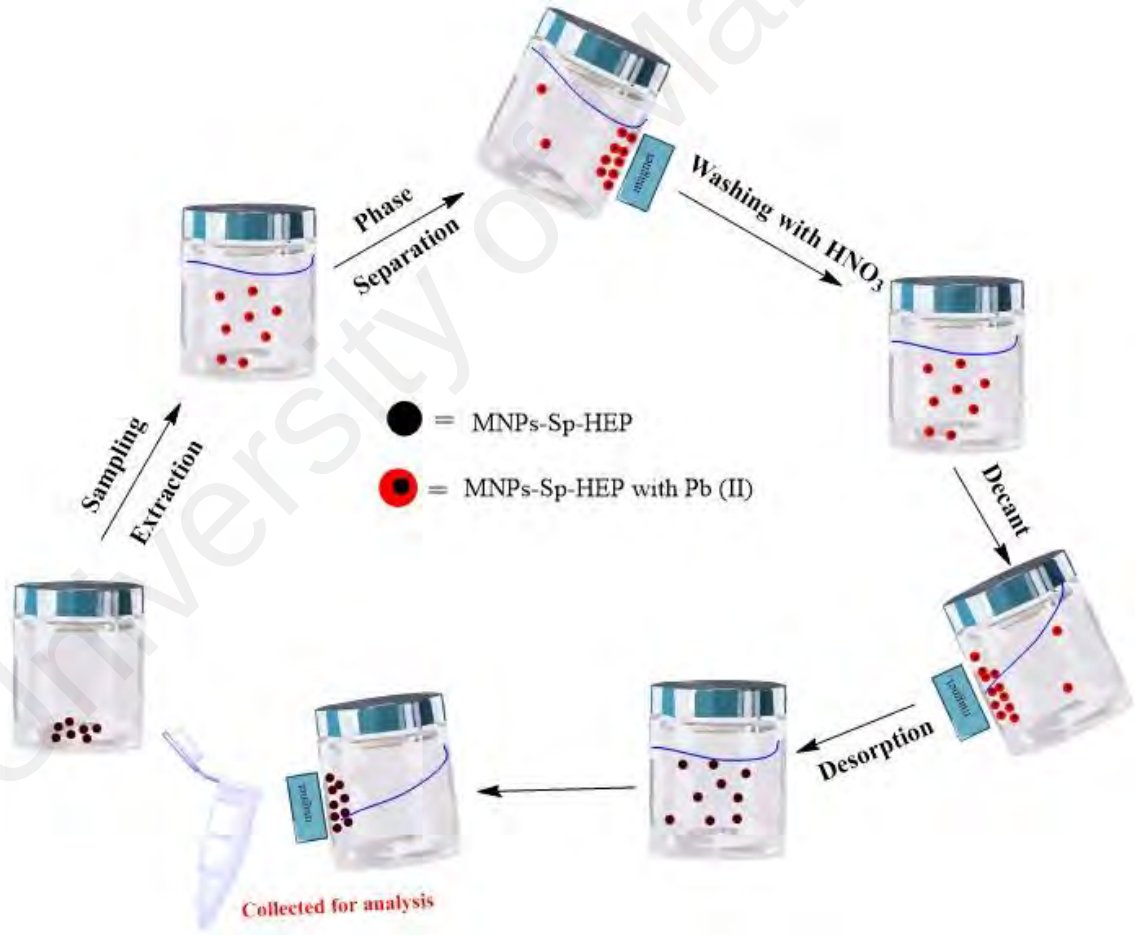

Figure 3.3 Schematic of determination procedure of Pb(II) ions by using MNPs-Sp-HEP

The percentage of recovery (%R) during optimization process was calculated by using the following formula:

$$\%R = \frac{C_f}{C_i} \times 100 \quad \textbf{(3.1)}$$

Where C_f and C_i are the concentration of final and initial.

3.8 Method Validation

In order to evaluate the figure of merit of the proposed technique, linearity, limit of detection (LOD), limit of quantification (LOQ) and repeatability were investigated under optimized conditions. The linearity was analyzed through the standard curve ranging from 0.0005 to 0.1 mg L^{-1} by diluting appropriate amounts of Pb(II) ions stock solution with distilled water and prepared in triplicate. The calibration curves were prepared using 10 spiking levels of analytes. For each level, three replicate experiments were performed. The method chosen for this study is a linear regression that can be exposed to model as:

$$y = mx + c \quad \textbf{(3.2)}$$

This model is used to determine the sensitivity *b* and the LOD and LOQ. Therefore, the LOD and LOQ can be stated as:

$$\mathrm{LOD} = \frac{3\ \mathrm{s.d}}{\mathrm{m}} \quad \textbf{(3.3)}$$

$$\mathrm{LOQ} = \frac{10\ \mathrm{s.d}}{\mathrm{m}} \quad \textbf{(3.4)}$$

where *s.d* is the standard deviation of the response and *m* is the slope of the calibration curve. The standard deviation of the response can be estimated by the standard deviation

of *y*-intercepts (Shrivastava and Gupta, 2011). Pre-concentration factor (P.F) can be calculated by the following equation:

$$\mathrm{P.F} = \frac{\text{Sample Volume}}{\text{Eluent Volume}} \quad \textbf{(3.5)}$$

The precision of the method was investigated by repeatability (intra-day) and intermediate precision (inter-day) of both standard and sample solutions. Precision was determined in seven replicates of Pb(II) ions on the same day (intra-day precision) and daily for 3 days (inter-day precision). Results were presented as RSD %.

$$\text{RSD } \% = \frac{\text{s.d}}{\text{mean}} \times 100 \quad \textbf{(3.6)}$$

3.9 Determination of Pb(II) ions in real environmental sample

The invented MSPE adsorbent was used in water samples collected in separate polyethylene bottles and covered with aluminum foil from landfill and river Selangor and a tap water in the laboratory (University Malaya) to evaluate the reliability of the proposed method for extraction and pre- concentration of the Pb(II) ions from the real sample. The bottles were first pre-cleaned using 5% HNO_3 solution, washed using water/acetone and dried. All samples were stored -4°C until analysis. All samples were analyzed with optimized MSPE condition (Section 3.7). Recovery was calculated using equation 3.1.

CHAPTER 4: RESULTS AND DISCUSSION

4.1 Synthesis and characterization of MNPs-Sp-HEP

The main goal of this study was to design a new organic-inorganic hybrid sporopollenin based magnetic nanomaterial, having heterocyclic core as well as amino functional groups and exploration of its extraction properties towards the selected Pb(II) ions. To achieve the desired goal, sporopollenin was modified with 3-cyanopropyltriethoxysilane. In second step amino functionality was achieved by the functionalization of *3*-cyanopropyltriethoxysilane modified Sporopollenin (CPTS-Sp**)** with 1-(2-hydroxyethyl) piperazine (HEP) in the presence of dry toluene. In order to acquire, the hybrid/magnetic nature the Sp-HEP was magnetized with Fe_3O_4 and the resultant hybrid MNPs-Sp-HEP was chosen as an adsorbent.

In this section, the synthesized MNPs-Sp-HEP adsorbent was characterized using FT-IR, FESEM, EDX, PXRD, and VSM.

4.1.1 Fourier Transfer Infra-Red (FTIR) Spectra

The FT-IR spectra of the sporopollenin and modified sporopollenin were shown in Figure 4.1 (a-d). The spectrum of raw sporopollenin (Figure 4.1a) shows the characteristic adsorption bands of hydroxyl groups (OH), a broad band ranging from 3200 cm^{-1} to 3400 cm^{-1}. The peaks at 2924 cm^{-1} and 2854 cm^{-1} were due to C-H symmetric and a symmetric stretching respectively. The peak shown at 1516 cm^{-1} was due to the C=C stretching vibration of the aromatic rings and the one at 1710 cm^{-1} was due to the C=O stretching vibration of a carboxylic group (Dyab *et al*., 2016). The spectrum of Sp-CPTS (Figure 4.1b) shows that the characteristics adsorption bands of cyano group (C≡N) and siloxane (Si-O-Si) group stretching at 2245 cm^{-1} and 1110 cm^{-1} respectively. The lower intensity of carboxylic group stretching in CPTS modified sporopollenin (Figure 4.1b) as compared to the raw sporopollenin (Figure 4.1a) might

be due to the modification process and it due to the attachment of CPTS on hydroxyl and carboxylic group (Figure 4.1b). The frequency of OH stretching vibration is Sp-CPTS is shifted to 3358 cm^{-1} from 3249 cm^{-1} (Sp) (Çimen *et al*., 2014). The successful functionalization of Sp-CPTS with 1-(2-hydroxyethyl) piperazine (HEP) can be explained on the bases of disappearance as well as shifting of some diagnostic stretching bands in IR spectrum of Sp-HEP (Figure 4.1c). The disappearance of cyano group (C≡N) in Sp-HEP spectrum (Figure 4.1c) confirms that HEP was functionalized with the cyano group (C≡N) and it is a qualitative evidence for the conversion of cyano group (C≡N) into (C=N) group. The frequency of secondary amine from HEP was observed at range 3313 cm^{-1} - 3318 cm^{-1} overlapping with OH functional group form sporopollenin (Figure 4.1c). The peaks at 3249 cm^{-1} and 1710 cm^{-1} in sporopollenin (Figure 4.1a) decreased drastically after immobilization of CPTS shows that the attachment of CPTS on hydroxyl and carboxylic group (Figure 4.1b) and after functionalized with HEP shift to 1647 cm^{-1} due to the presence of an amine (Figure 4.1c). Moreover, the sharp peak at 564 cm^{-1} may be attributed to nanoparticles (Fe_3O_4) groups obtained when Sp-HEP was coated with Fe_3O_4 (Figure 4.1d) (Arora *et al*., 2016).

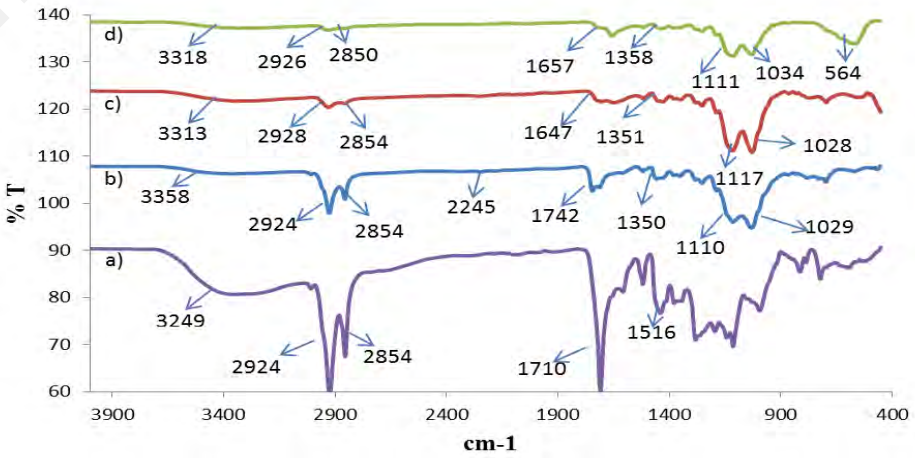

Figure 4.1 FT-IR spectrum of (a) raw sporopollenin (b) Sp-CPTS, (c) Sp-HEP and(d) MNPs-Sp-HEP

4.1.2 Field Emission scanning electron microscope (FESEM)

Surface morphology images of pure sporopollenin and MNPs-Sp-HEP (Figure 4.2) revealed that raw sporopllenin consists of a uniform interconnected hexagonal shape pore structure (in the form of round microcapsule). The open and uniform pore structure of modified sporopollenin showed a distinct roughness pattern due to the functionalization/magnetization with HEP and MNPs respectively, non-uniformly deposited inside the pores and on the pore walls. It can be seen from Figure 4.2, that each pore of sporopollenin remained hollow even after modification, functionalization as well magnetization process and thus will help to enhance the adsorption process (Tutar *et al*., 2009).

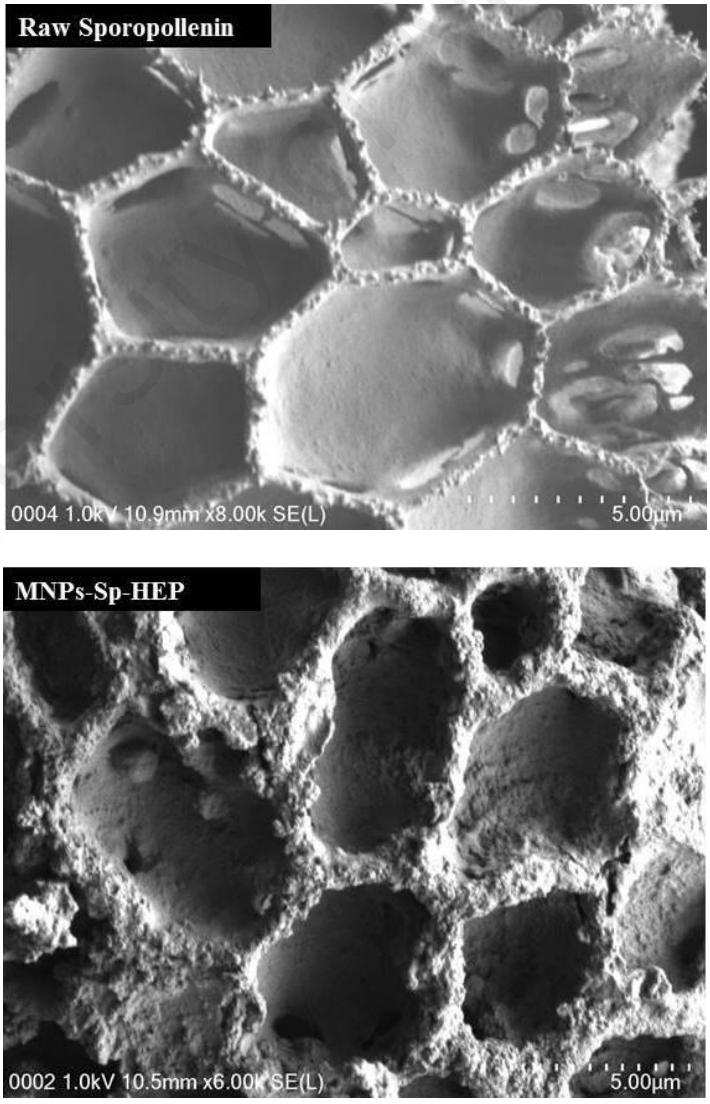

Figure 4.2 FESEM images of raw sporopollenin and MNPs-Sp-HEP

4.1.3 Energy dispersive X-ray (EDX)

The pureness and elemental composition of sporopollenin and functionalized sporopollenin were investigating using EDX. The functionalized sporopollenin was compared with raw sporopollenin. Table 4.1 shows the elemental composition for raw sporopollenin, Sp-CPTS, Sp-HEP and MNPs-Sp-HEP. The presence of additional nitrogen, silica and iron on functionalized sporopollenin show that they are successfully functionalized/magnetize onto sporopollenin as the natural composition of sporopollenin spores are only form hydrogen, carbon and oxygen (Chiappe *et al*., 2017).

Table 4.1 EDX result of modified sporopollenin**.**

Element	Sp	Sp-CPTS	Sp-HEP	MNPs-Sp-HEP
C	73.25	69.41	76.79	58.76
O	26.75	23.58	16.68	25.52
N		2.02	4.45	3.55
Si		4.99	2.05	2.59
Fe				9.57

4.1.4 X-Ray Difractometer (XRD)

Further evidence for the formation of MNPs-Sp-HEP was obtained through the XRD analysis, as demonstrated in Figure 4.3. There were five main diffraction peaks found at $2\theta = 31.8°$, 34.3°, 45.4°, 55.3° and 62.4° that indicates a good crystallinity of Fe_3O_4 nanoparticles. A broad diffraction was observed at $2\theta \sim 20\theta$ ° related to the presence of amorphous materials which is sporopollenin. Hence, in this study, it had been confirmed that the iron oxide nanoparticles were embedded inside the sporopollenin.

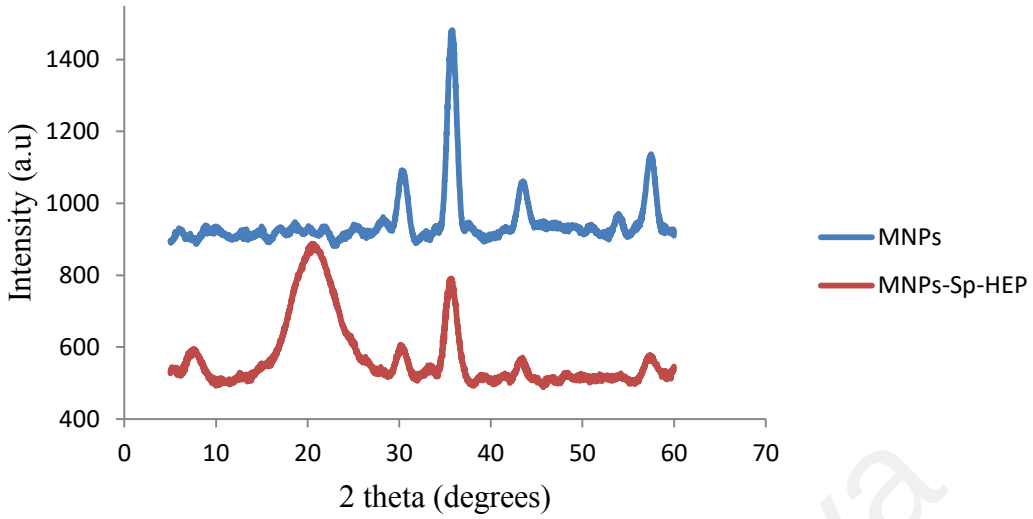

Figure 4.3 XRD pattern of MNPs (blue) and MNPs-Sp-HEP (red)

4.1.5 Vibrating sample magnetometer (VSM) analysis

Magnetic properties were characterized by measuring the hysteresis and remanence curves by means of VSM. Figure 4.4 shows the magnetization curves of MNPs and MNPs-Sp-HEP. The two curves show similar symmetrical about the original shape which exhibits the characteristics feature of superparamagnetic. The MNPs achieved a saturation magnetization value of 63.3 emu g^{-1} similar to that obtained from the literature (Baharin *et al*., 2016). After functionalized with Sp-HEP, the saturation magnetization value dropped significantly (15.64 amu g^{-1}). This was predicted due to the coating contribution from a non-magnetic functionalized sporopollenin. However, the decreases of saturation magnetization give no significant difference between the two superparamagnetic properties of MNPs which is sufficient for magnetic separation with a conventional magnet (Zheng *et al*., 2014).

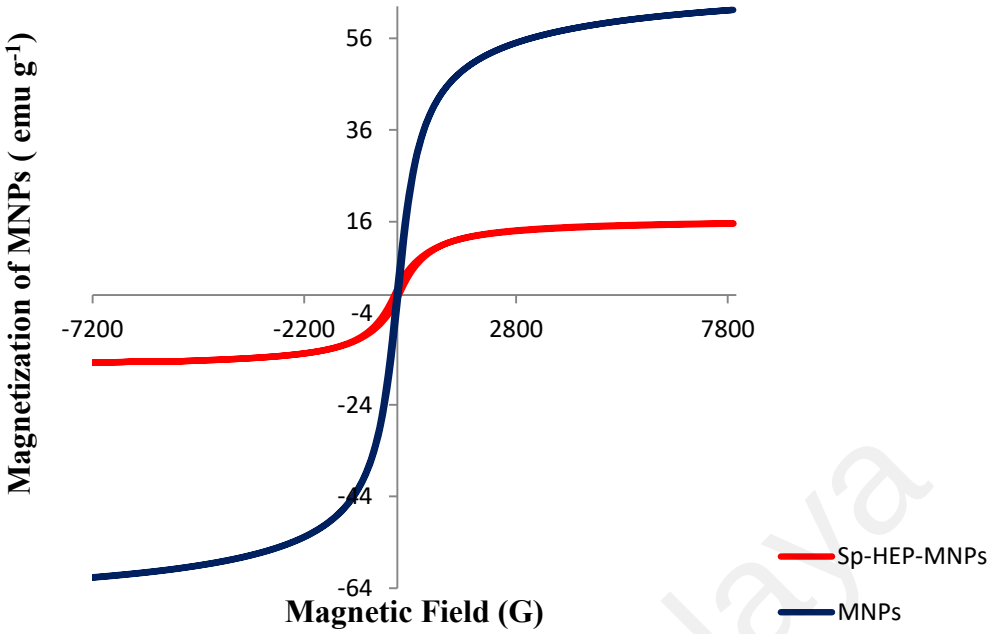

Figure 4.4 The magnetic behavior of MNPs (blue) and MNPs-Sp-HEP (red).

4.2 Adsorption Study

4.2.1 Screening Study

Synthesized sample is applied in sorption studies in order to compare the performance of this sorbent with Sp and MNPs. The efficiency of the sorbents for the removal of Pb(II) ions is presented in Figure 4.5**.** It was found that the MNPs-Sp-HEP enhance the efficiency of removal of Pb(II) ions compared to the other sorbents. This can be explained by the combined properties of MNPs and modified sporopollenin with 1-(2-hydroxyethyl) piperazine which enhances the ability and selectivity of MNPs-Sp-HEP towards Pb(II) ions. According to hard and soft (Lewis) acids and bases (HSBA) concept, Pb(II) ion is more prone to the adsorbent with more amine group as in MNPs-Sp-HEP, compared to the other sorbents. Since the MNPs-Sp-HEP has demonstrated the highest percentage (%) removal of Pb(II) ions, it was selected for further adsorption and MSPE optimization.

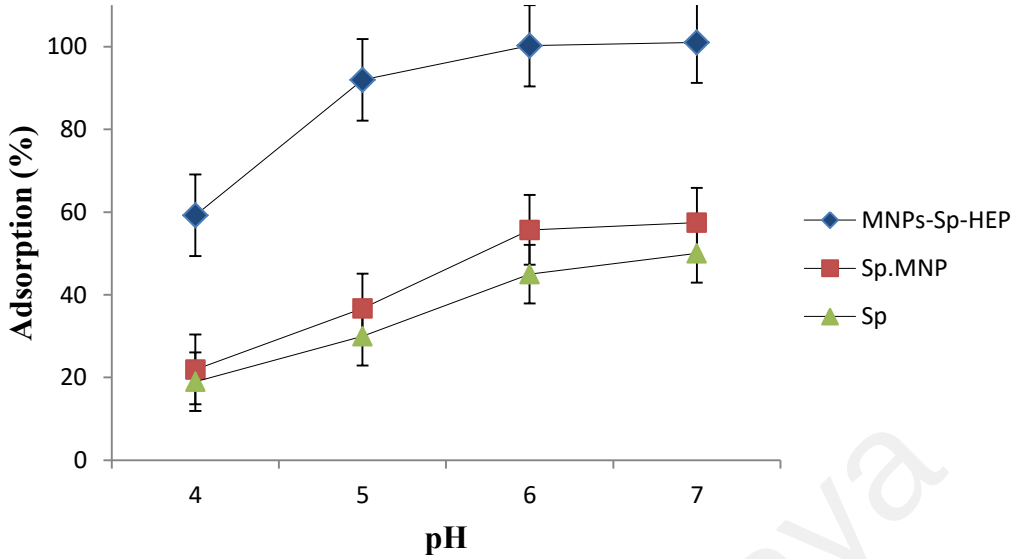

Figure 4.5 Percent of adsorption of Pb(II) ions on different type of adsorbents

4.2.2 Adsorption of studies of Pb(II) ions on MNPs-Sp-HEP

Effect of adsorbent dosage

The amount of adsorbent is important to achieve maximum removal of Pbs(II) ions from water sample thus; the dosage of synthesized material was investigated. Five different amount (10 mg – 50 mg) were used for the adsorption of 10 mg L^{-1} of Pb(II) ions from 10 mL water sample at pH 6.5 since, at pH 6.5, the efficiency is the highest (> 95%). The adsorption efficiency of Pb(II) ions is directly proportional to the mass of adsorbent due to an increase in adsorption sites and thus, more analyte can occupy these sites. Beyond the 25 mg of the adsorbent dosage, there is no significant increase and adsorbent becomes almost constant. The result indicated that MNPs-Sp-HEP has reached the adsorption equilibrium, where the maximum capacity of the adsorbent was reached. Consequently, 25 mg was selected for the subsequent experiment (Figure 4.6).

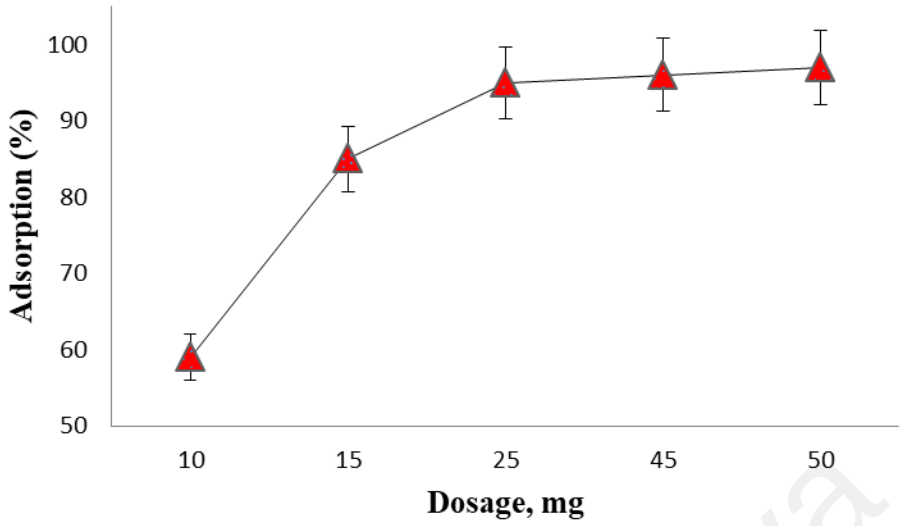

Figure 4.6 Effect of adsorbent dosage on percentage of adsorption

4.2.2.2 Effect of the pH of the solution

The pH of the adsorbate solution has influence on the whole adsorption capacity, the surface charge and the ionization of the functional groups on the adsorbent, and the degree of ionization of the molecules in solution. H^+ and OH^- are usually strong adsorbed and therefore, the adsorption of other ions is affected by the solution pH.

The pH of the solution plays an important role in the adsorption characteristic of Pb(II) ions. Only pH between 3.5– 6.5 are tested because at pH above 7, Pb(II) ions will form precipitate which is lead oxide (Escudero *et al*., 2013). Figure 4.7a displays the removal of Pb(II) ions at different pH values. The increase of the pH of the solution up to pH 6.5 increased the percentage removal of Pb(II) ions due to the electrostatic interaction between Pb(II) ion and negatively charged surfaces. Significant 95% was acquired at pH 6.5. The lower percentage removal of Pb(II) ions at low pH might be due to the competition between Pb^{2+} and H^+ with active sites and repulsion of Pb^{2+} and protonated amine. After this point, based on zeta potential result (Figure 4.7b) at higher pH, surface of the adsorbent become more negatively charge due to deprotonation of C=N and acidic group of particle surfaces (Binks *et al*., 2011).

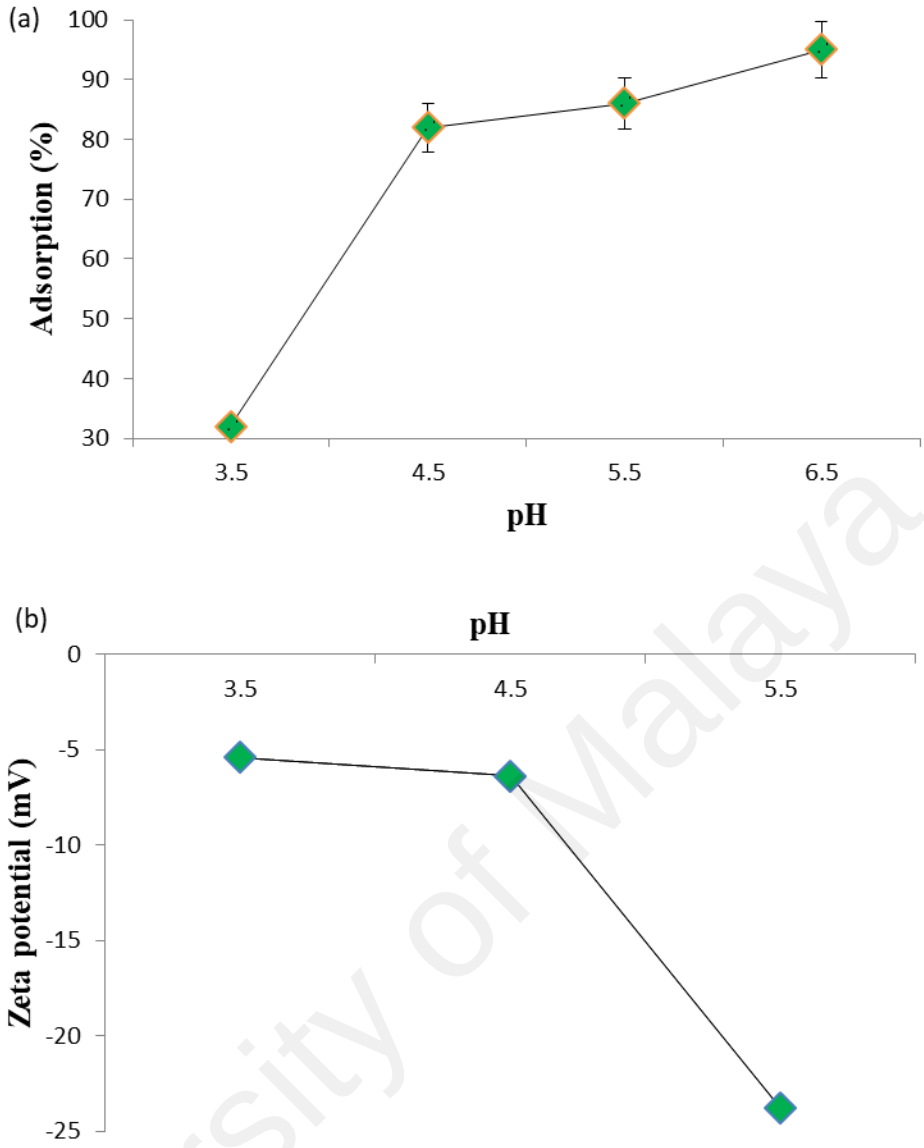

Figure 4.7 (a) Effect of solution pH (b) The zeta potential of MNPs-Sp-HEP at various pHs

4.2.2.3 Effect of contact time of adsorbent onto target analyte

The performance of adsorption method was also evaluated for adsorption time to achieve the highest removal. In this regard, adsorption time trials ranging from 5 to 25 min were studied (Figure 4.8). The highest percent removal for Pb(II) ions was observed for 15 min adsorption time. After 15 min adsorption time, the amount of Pb(II) ions adsorbed become constant probably due to the all adsorption site on 25 mg of MNPs-Sp-HEP were saturated.

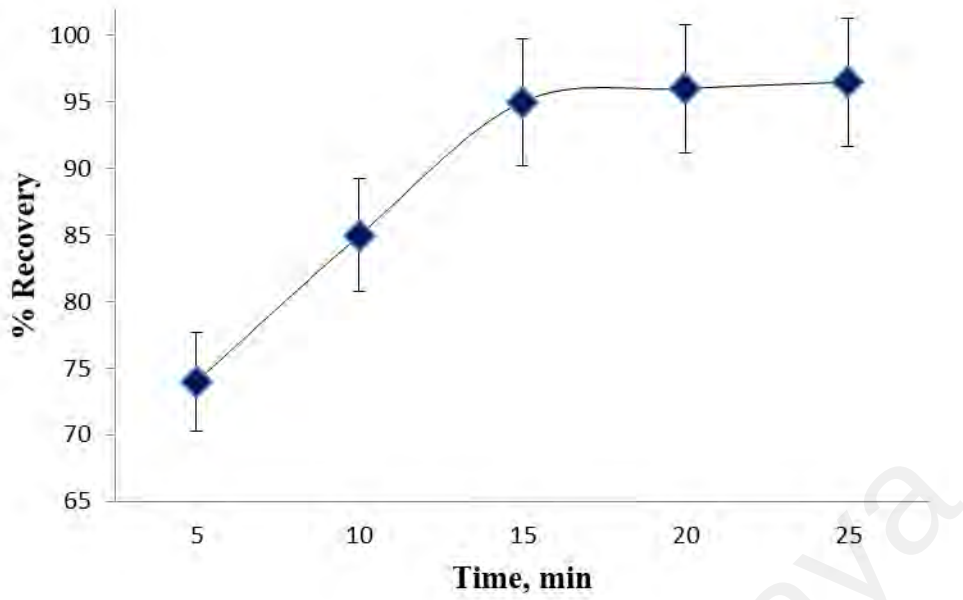

Figure 4.8 Effect of contact time adsorbent onto Pb(II) ions

4.2.2.4 Adsorption kinetics

Different kinetic models were carried out to study the time required for the adsorption equilibrium to be reached and condition under which there is no variation in adsorption capacity. In this study, the pseudo-first order, pseudo second-order kinetic and intraparticle diffusion models were applied to the kinetic adsorption data to find the best-fitted model for the experimental data.

(i) ***Pseudo first order kinetic model***

The pseudo-first order model proposed that as time progress, the sorbate ions are accumulating over the surface of sorbent (Daraei *et al*., 2015; Ho, 2006). This is shown in Figure 4.9a

The pseudo first- order equation is expressed as:

$$ln\ (q_e - q_t) = ln\ q_e - k_1 t \qquad (4.1)$$

In the equation above, q_e and q_t are the amounts of Pb(II) ions (mg g^{-1}) absorbed at

equilibrium and at the time, *t,* respectively and k_1 is the first-order rate constant (min^{-1}). The values of q_e and k_1 were obtained from the linearity of pseudo first-order rate by plotting $ln\ (q_e - q_t)$ versus time (Figure 4.9b).

(ii) ***Pseudo second order kinetic model***

A pseudo second-order kinetic model which has been applied for analyzing chemisorption kinetics from liquid solutions can be represented by Eq. (4.2) as follow:

$$\frac{t}{q_1} = \frac{1}{k_2 q_e^2} + \frac{t}{q_e} \tag{4.2}$$

Where the k_2 is the rate constant of pseudo second-order adsorption (g/mg min). The value of k_2 and q_e can be described from the slope and the intercept of the graph t/q_t versus t (Figure 4.9c), respectively.

By comparing the R^2 value from both first order and second order kinetics (Table 4.2), it can be concluded that the experimental data followed pseudo second-order kinetic and involves chemisorption mechanism which indicates that the adsorption process is driven by a chemical reaction occurring at the exposed surface.

Sporopollenin has a porous structure, therefore the adsorption process on porous sorbents was described by intraparticle diffusion; where in mass transfer within the sorbent particles may involve a short-range diffusion in both the fluid and adsorbed phase (Nair *et al*. 2012; Unlü and Ersoz 2006).

The model is expressed with the equation given by Weber and Morris.

$$q_t = k_{id}\, t^{1/2} + C_i \tag{4.3}$$

Where q_t and k_{id} is the amount of metal ions adsorbed at time t and intraparticle diffusion rate constant, respectively. Whereas, C_i is the intercept which gives the idea

about the thickness of the boundary layer. Intraparticle diffusion values (Table 4.2) were obtained from linearity of q_t versus $t^{1/2}$ plot. Figure 4.9d shows two part linearity i.e. mass transfer (first stage) and equilibrium part (second stage) for intra-particle diffusion model revealed that Pb(II) ions adsorption was conducted in two separate regions with two straight lines. The first part with a sharp slope showed that the adsorption rate is fast and adsorption is favorable on the surface. The second part with slow slope shows that the adsorption rate is slow due to diffusion of Pb(II) ions through the MNPs-Sp-HEP (Jalil *et al*., 2010).

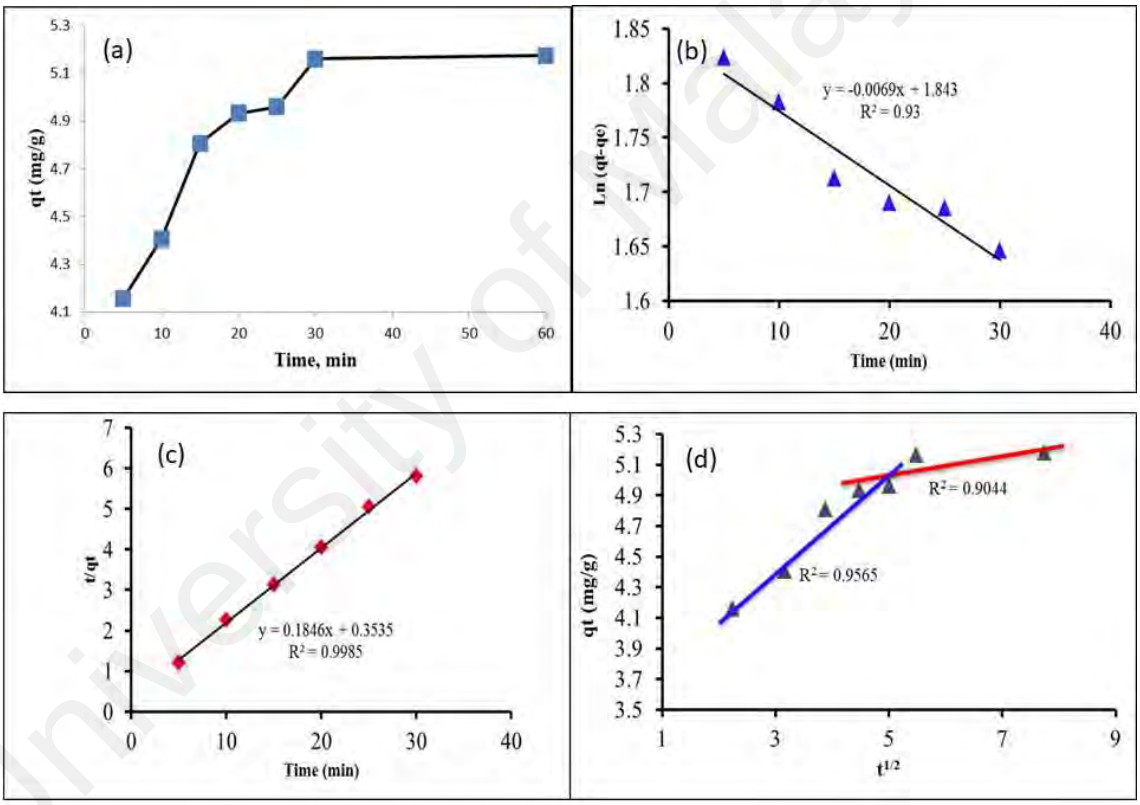

Figure 4.9 (a) Experimental contact time: Plot of qt (mg g-1) versus time for the adsorption.of Pb(II) ions on MNPs-Sp-HEP (b) is linearity of pseudo-first-order rate .model (c) is linearity of pseudo-second-order rate model and (d) is intra-.part

Table 4.2 Kinetic modeling constants and coefficient of determination for adsorption of.Pb(II) ions on Sp-HEP-MNPs

Model / Isotherm constant	Equation / Value
Pseudo- first- order	$\text{Ln}\ (q_e - q_t) = \text{Ln}\ q_e - k_1 t$
k_1 (min^{-1})	-0.0069
q_e (mg g^{-1})	6.26
R_1^2	0.93
Pseudo second order	$t/q_t = 1/k_2\ q_e^2 + 1/q_e$
k_2 (g mg^{-1} min^{-1})	0.096
q_e (mg g^{-1})	5.43
R_2^2	0.99
Intraparticle diffusion	$q_t = k_{id} t^{1/2} + C_i$
$K_{id,\ 1}$	0.38
C_1	3.2
R_1^2	0.9565
$K_{id,\ 2}$	0.2
C_2	4.04
R_2^2	0.9044

4.2.2.5 Effect of the concentration of adsorbent onto target analyte

Adsorption isotherms describe how adsorbate interacts with the adsorbents and therefore, it is a priority to optimize the design of an adsorption process. Hence, it is essential to establish the most appropriate correlation for the equilibrium curve. Over the years, a wide variety of equilibrium isotherm models has been formulated in terms

of three fundamental approaches. Langmuir and Freundlich isotherms are the most frequently used models and were investigated in this work.

(i) ***Langmuir isotherm***

Langmuir adsorption isotherm originally developed to describe gas–solid-phase adsorption onto activated carbon, has traditionally been used to quantify and contrast the performance of different bio-sorbents. In its formulation, this empirical model assumes monolayer adsorption (the adsorbed layer is one molecule in thickness), with adsorption can only occur at a finite (fixed) number of definite localized sites, that are identical and equivalent, with no lateral interaction and steric hindrance between the adsorbed molecules, even on adjacent sites. Langmuir isotherm refers to homogeneous adsorption, which each molecule possess constant enthalpies and sorption activation energy (all sites possess an equal affinity for the adsorbate), with no transmigration of the adsorbate in the plane of the surface (Chou *et al*., 2011). Therefore, at equilibrium, a saturation point is reached where once a molecule occupies a site, no further adsorption can take place.

The Langmuir isotherm is represented by following equation:

$$\frac{C_e}{q_e} = \frac{C_e}{q_m} + \frac{1}{q_m b} \tag{4.4}$$

Where q_e is the amount of solute sorbed on the surface of the sorbent, C_e is the equilibrium ion concentration in the solution, q_o is the maximum surface density at monolayer coverage, and b is the Langmuir adsorption constant. The plot of $\frac{C_e}{q_e}$ vs. C_e for the sorption gives a straight line of slope $\frac{1}{q_o}$ (Figure. 4.10).

The isotherm equation further assumes that the adsorption takes place at specific homogenous sites within the adsorbent. It is then assumed that once a metal ion

occupies a site, no further adsorption can take place at that site. Theoretically, the sorbent has a finite capacity for the sorbate (El-Geundi *et al*., 2012). The Langmuir isotherm assumes that metal ions are chemically adsorbed at a fixed number of well-defined sites, where each site can hold only one ion, and all sites are energetically equivalent without any interaction between the ions (Igwe and Abia 2007).

Figure 4.10 shows the plot of adsorption isotherm in Langmuir model sorption with correlation coefficient R^2 is >0.9. The values of q_m and b for Langmuir isotherm are listed in Table 4.3. It was found that the plot is linear with good correlation coefficient.

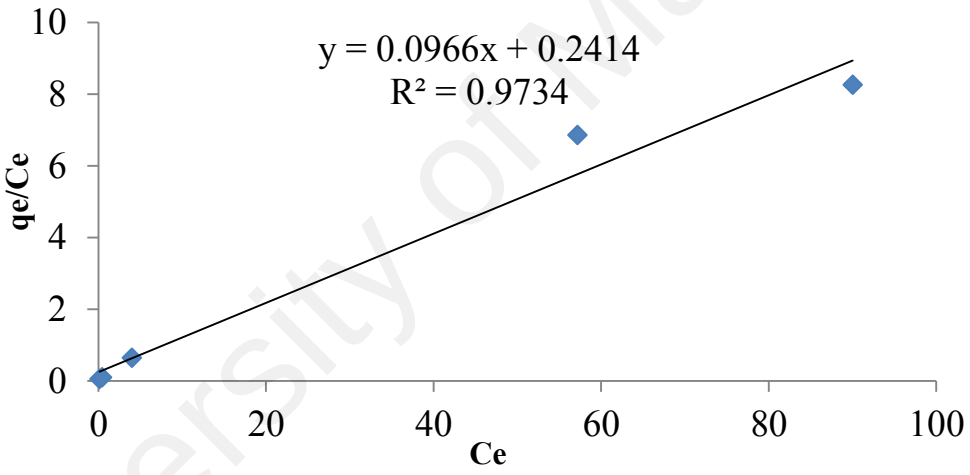

Figure 4.10 Langmuir isotherms of removal of Pb(II) ions by MNPs-Sp-HEP.

(ii) ***Freundlich isotherm***

Freundlich isotherm describing the non-ideal and reversible adsorption, not restricted to the formation of a monolayer. This empirical model can be applied to multilayer adsorption, with non-uniform distribution of adsorption heat and affinities over the heterogeneous surface. The amount adsorbed is the summation of adsorption on all sites (each having bond energy), with the stronger binding sites are occupied first until adsorption energy is exponentially decreased upon the completion of the adsorption

process. At present, Freundlich isotherm is widely applied in heterogeneous systems especially for organic compounds or highly interactive species on activated carbon and molecular sieves (Fadzil *et al*., 2016). The slope ranges between 0 and 1 is a measure of adsorption intensity or surface heterogeneity, becoming more heterogeneous as its value gets closer to zero. Whereas, a value below unity implies chemisorptions process where 1/n above one is an indicative of cooperative adsorption.

Freundlich model is an empirical equation which can be written as:

$$Ln\ q_e = Ln\ K_F + \frac{1}{n} Ln\ C_e \qquad (4.5)$$

Where K_F and *n* are Freundlich constant related to the adsorption capacity and adsorption intensity, respectively. q_e is the equilibrium solute concentration on the adsorbent, C_e is the equilibrium concentration of the solute. According to Eq. (4.5), the plot of ln $q_e$vs. ln C_e gives a straight line, and K_F and *n* values can be calculated from the intercept and slope of this straight line (Figure 4.11).

Based on the calculation, Freundlich model showed that theoretical q_e was comparable with experimental q_e because the exponent is between $1 < n < 10$. This trend showed favorable adsorption for Pb(II) ions onto MNPs-Sp-HEP adsorbent.

The calculated parameters of Langmuir and Freundlich isotherms and the corresponding correlation coefficients (R) are listed in Table 4.3. These results show that experimental data follow the Langmuir model according to R^2. Therefore, the data fit the Langmuir isotherm satisfactorily.

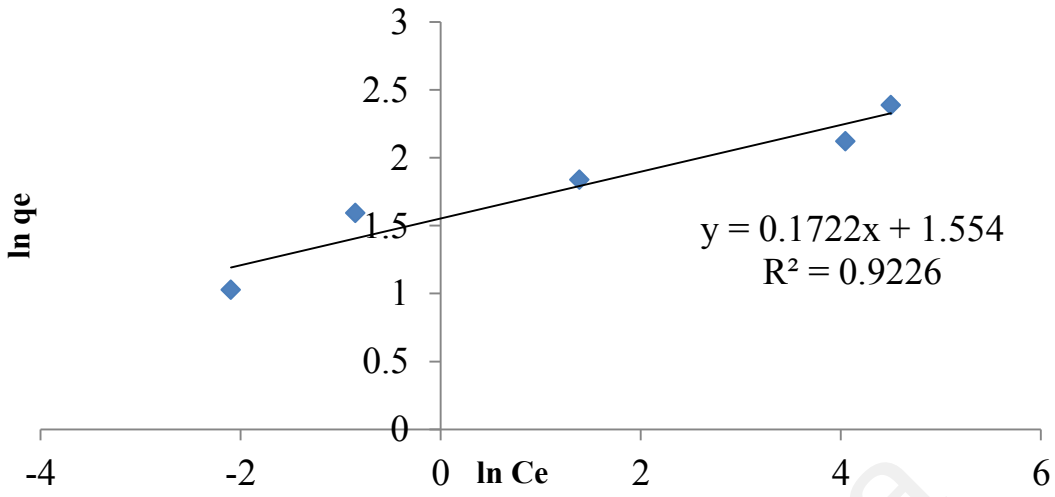

Figure 4.11 Freundlich isotherms of removal of Pb(II) ions by MNPs-Sp-HEP

Table 4.3 Langmuir and Freundlich model constants and coefficient of determination for adsorption of Pb(II) ions on MNPs-Sp-HEP.

Models	Equation	Isotherm constant	Pb(II)
Langmuir	$\frac{C_e}{q_e} = \frac{C_e}{q_m} + \frac{1}{q_m b}$	q_m (mg g^{-1})	10.35
		b (L mg^{-1})	0.48
		R^2	0.97
Freundlich	$\text{Ln } q_e = \text{Ln } K_F + \frac{1}{n} \text{Ln } C_e$	K_F [(mg/g) / $(mg/g)^{1/n}$]	4.26
		N	5.81
		R^2	0.92

4.2.2.6 Thermodynamic studies

The adsorption thermodynamics were studied to gain an insight into the effect of temperature on the adsorption behaviors. The temperature was studied at 293, 303 and 313 K and the equilibrium adsorption capacity (mg g^{-1}) was calculated using equation. The adsorption capacity is increased with an increased in temperature. According to (Kumar *et al*., 2014), the trend is probably due to the increasing in diffusion and

decreased in viscosity of the solution. The increasing q_e values indicate that the nature of adsorption process is endothermic.

Parameters that can explain the mechanism of adsorption process, including enthalpy change (ΔH°), entropy change (ΔS°) and Gibbs free energy change (ΔG°) are calculated according to the following thermodynamic equations:

$$\Delta G° = -RT \ln K \quad (4.6)$$

$$\ln K = \frac{\Delta S°}{R} - \frac{\Delta H°}{RT} \quad (4.7)$$

where K (L/mol) is from Langmuir equation, R is the gas constant (8.314 J/mol K) and T is the temperature in Kelvin. In the application of Eq. (4.7), the values of ln K are plotted against 1/T, the ΔH° and ΔS° values are calculated from the slope and intercept of the plot.

The thermodynamic parameters are listed in Table 4.4. Negative ΔG° values are obtained at a different temperature, revealing the adsorption process is feasible and spontaneous and required energy from outside of the system. As the temperature increase, the value of ΔG° is decreasing suggesting that the spontaneous nature of adsorption was inversely proportional to temperature.

The negative values of ΔH°, demonstrating the exothermic nature of adsorption and the positive values of ΔS° suggest the organization of the adsorbate at the solid/ solution interface becomes more random as ion replacement reaction occurred, while negative value suggests the opposite fact (Alothman *et al*., 2016; Daraei *et al*., 2015).

Table 4.4 Thermodynamic parameters for sorption of Pb(II) ions of MNPs-Sp-HEP

Temperature (K)	ΔG° kJ mol^{-1}	ΔH° kJ mol^{-1}	ΔS° J mol^{-1} K^{-1}
293	-2.73		
303	-4.12	-47.47	0.17
313	-6.16		

4.2.2.7 Proposed mechanism

The adsorption mechanism of Pb(II) ions metal ions on MNPs-Sp-HEP was explained in Figure 4.12. Since MNPs-Sp-HEP contains nitrogen and oxygen groups, these N and O groups are highly electronegative due to the abundance of a free lone pair of electrons. These lone pair electrons show binding abilities towards the Pb(II) ions as represented in Figure 4.12.

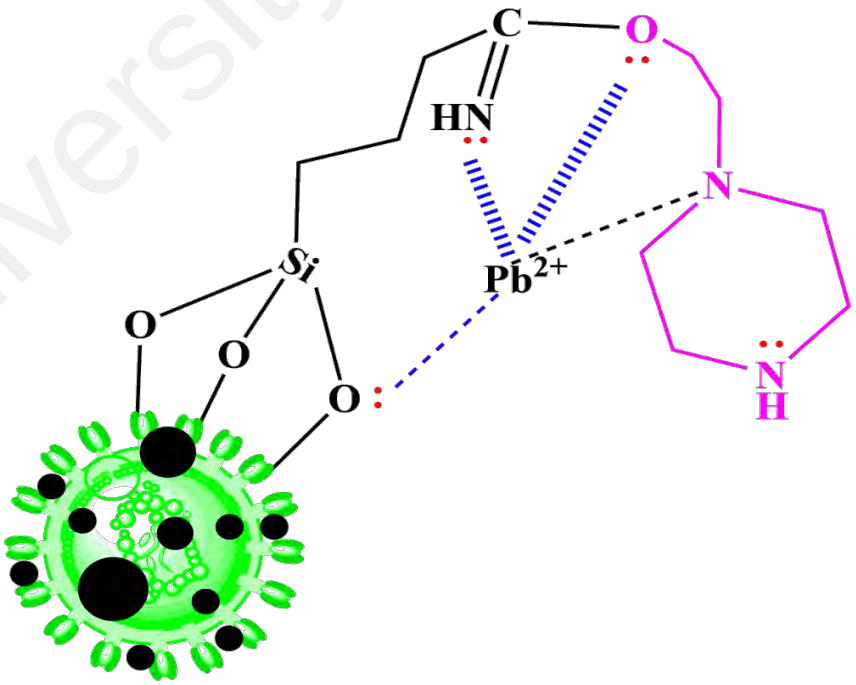

Figure 4.12 Proposed mechanism of interaction between Pb(II) ions and MNPs-Sp-HEP

4.3 The application of MNPs-Sp-HEP as adsorbent in MSPE study

4.3.1 Optimization of the MSPE condition

The MSPE technique is based on two steps: the first one is the adsorption of the Pb(II) ions from the sample solution, and the second step is the elution of the adsorbed Pb(II) ions from MNPs-Sp-HEP surface with suitable eluent. The following parameters were optimized: (a) Sample volume; (b) Eluent concentration and volume; (c) contact time for loading and unloading Pb(II) ions solution.

4.3.1.1 Effect of sample volume

According to Wan Ibrahim *et al*., (2012), the sample volume is important in extraction procedure because the recovery of analyte, intensity and enrichment factor achieved depend on the sample volume. Five different sample volume ranging from 20 – 180 mL were studied in 0.1 mg L^{-1} Pb(II) ions followed by the addition of 25 mg of adsorbent and 15 minutes shaking time at pH 6.5. The recovery of Pb(II) ions increased slowly up to 140 mL sample volume and then decreased at 180 mL (Figure 4.13). An increase in sample volume could lead to a high distribution of adsorbent to the aqueous phase, which lowered the amount of adsorbent in the volume unit sample solution, and the extraction becomes less effective (Tahmasebi *et al.*, 2013). Thus, 140 mL was selected as the optimum sample volume for Pb(II) ions pre-concentration.

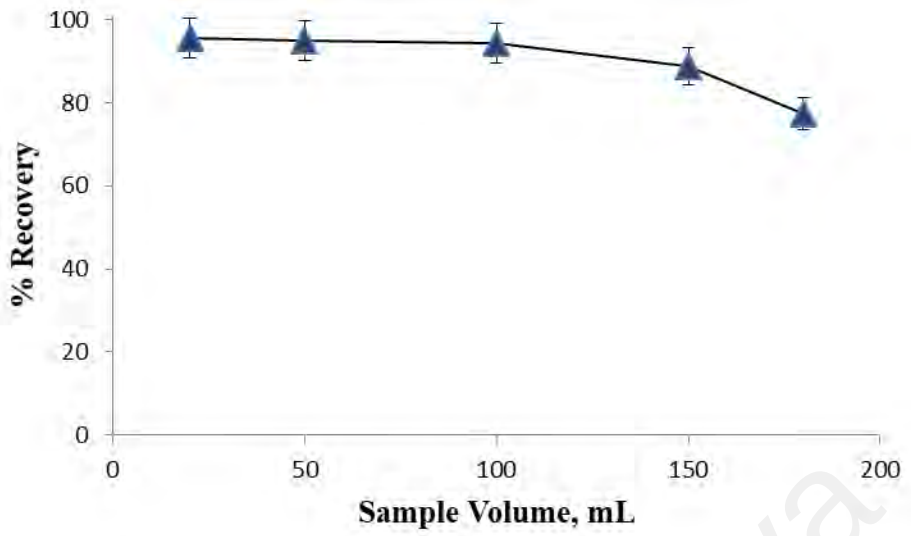

Figure 4.13 Effect of sample volume on recovery (%). (Optimum conditions: dosage.= 25 mg, time = 15 minutes and pH = 6.5)

4.3.1.2 Effect of volume and concentration of HNO_3

HNO_3 does not form any insoluble compounds with metals and non-metals, whereas H_2SO_4 and HCl do (Zhang, 2007). Therefore, HNO_3 was chosen as eluent for Pb(II) ions for MSPE.

The volume of desorption solvent was studied using four different volumes of 0.3 mol L^{-1} of HNO_3 are 1-4 mL. The extraction efficiency depends entirely on the analytes desorbed from the adsorbent. There was a small increase with increasing volume of desorption solvent from 1 to 3 mL. (Figure 4.14a). Thus, 3 mL of HNO_3 was selected as the best desorption solvent volume prior to FAAS analysis.

Figure 4.14b showed the effect of concentration of HNO_3 on the recovery of the target analyte. The capability to remove more metals as increase the concentration of acid. As could be seen, quantitative recovery for Pb(II) ions could be obtained with 0.3 mol L^{-1} HNO_3 and this oncentration was chosen for further experiment.

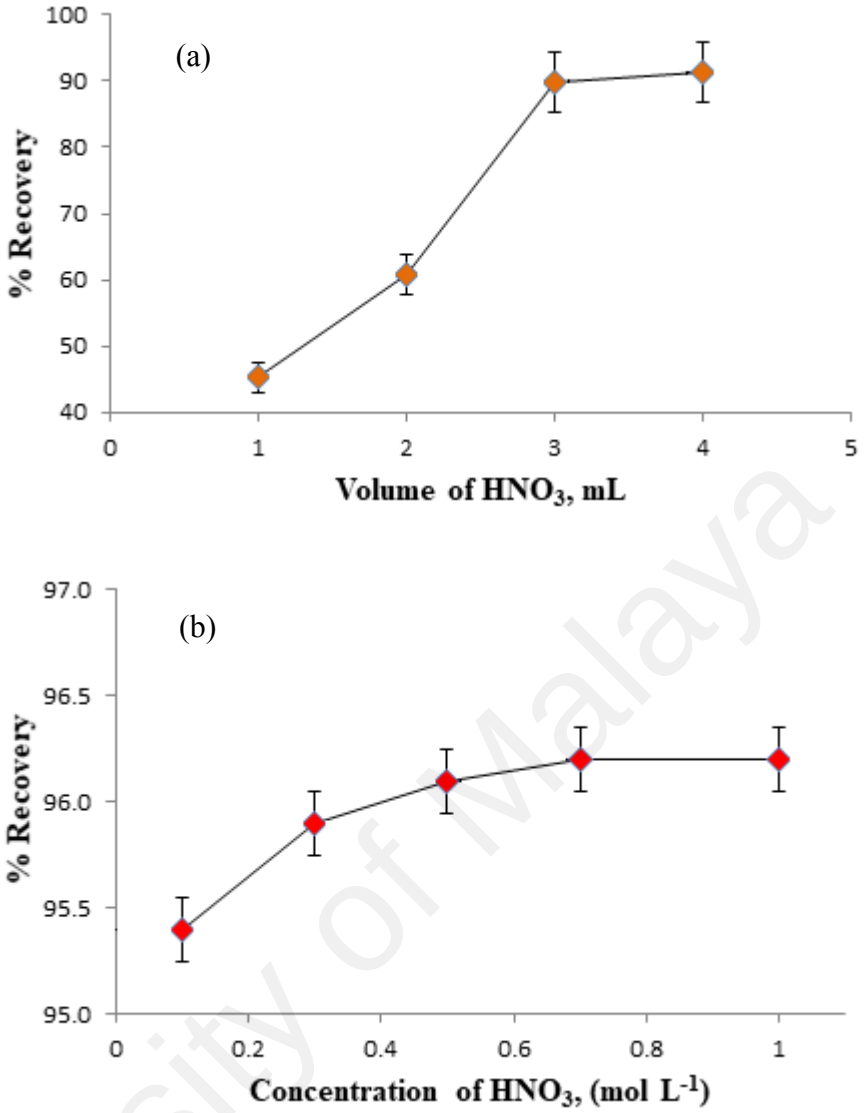

Figure 4.14 Effect of (a) volume and (b) concentration of HNO3 on the recovery of the Pb(II) ions on MNPs-Sp-HEP. (Optimum conditions: Dosage = 25 mg of MNPs-Sp-HEP, sample volume = 140 mL, elution volume = 3 mL of 0.3 mol L-1 NHO3, time = 15 minutes and pH tested = 6.5)

4.3.1.3 Effect of extraction and desorption time

It has been understood that prolonged extraction time might increase the recovery (%) of analytes. Thus, the influence of extraction time on the recoveries of the analyte has been investigated. As demonstrated in Figure 4.15, the recovery (%) increased rapidly for the first 15 minutes, since more adsorption sites were available and Pb(II) ions could easily interact with these sites. After 15 minutes, the recovery (%) was

persistent; therefore, 15 minutes was sufficient to extract the maximum of the target analytes.

Further, desorption time was optimized to investigate the best time taken for the analytes to desorb from the sorbent ranging from 5- 25 min. As reveals in Figure 4.15, analytes were desorbed rapidly in the first 10 min and started to become constant after 10 min. This indicated that 10 min of time is sufficient to desorb back all of the analytes from the adsorbent.

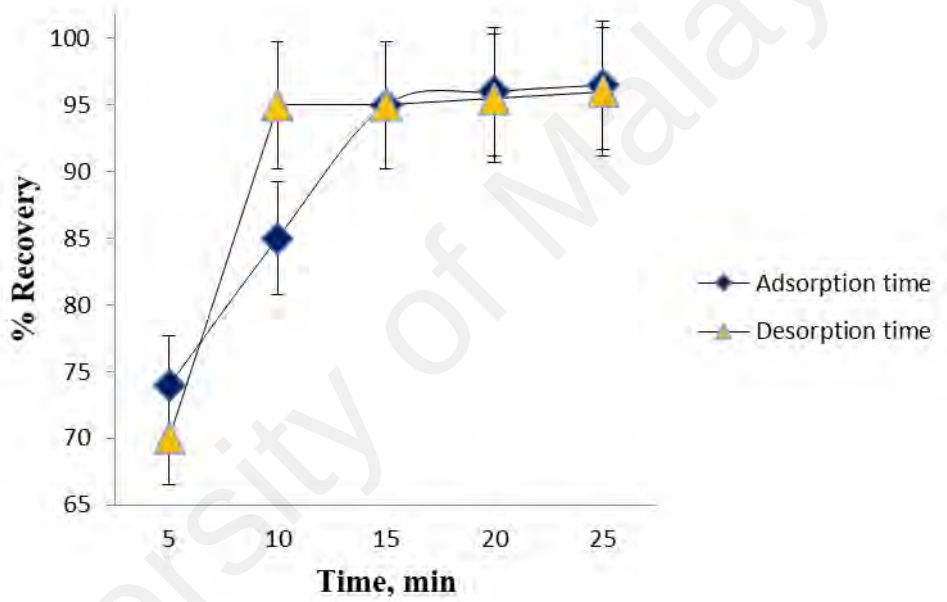

Figure 4.15 Effect of adsorption and desorption time on recovery (%). (Optimum conditions: Dosage = 25.mg of MNPs-Sp-HEP, sample volume = 140 mL, elution volume = 3 mL of 0.3 mol L-1 NHO3, adsorption time = 15 minutes, desorption time = 10 minute and pH tested =6.5)

4.3.2 Interferences ion

Matrix effect is a critical problem in the determination of metals in real samples. Under optimized condition, the interference of common cations and anions on the recovery of Pb(II) ions was investigated. Potentially seven interfering ions (0.5 mg L^{-1}) were added to test solutions containing 0.1 mg L^{-1} Pb(II) ions. The sample was then treated according to the above mentioned MSPE procedure (Section 3.7). The result

(Table 4.5) indicates that the method could be successfully applied to the extraction of Pb(II) ions from complicated real matrices with high selectivity toward the Pb(II) ions.

Table 4.5 Effect of interference ions on pre-concentration and determination of Pb(II) ions.

Interference ions	Recovery %
K^+	94
F^-	95
Cl^-	98
Zn^{2+}	95
Mg^{2+}	91
SO_4^{2-}	90
Fe^{3+}	94
Pb^{2+} without interference ions	96

4.3.3 Regeneration of MNPs-Sp-HEP

Due to the stability of MNPs-Sp-HEP under acidic conditions, Pb^{2+} loaded adsorbent was regenerate using 0.3 M HNO_3 solution and the regeneration adsorbent was reused in adsorption in seven consecutive cycles (n=7). Adsorption efficiency of the regenerated adsorbents was shown in Figure 4.16a. The adsorption capacity had decreased slightly by first five adsorption- regeneration capacity cycle, and drastically dropped at cycle five. This might be due to the partial breakup of outer MNPs-Sp-HEP shell and cell walls at high concentration of nitric acid (Şener *et al.,* 2014) as confirmed by FT-IR analysis (Figure 4.16b) of the MNPs-Sp-HEP after seven cycles.

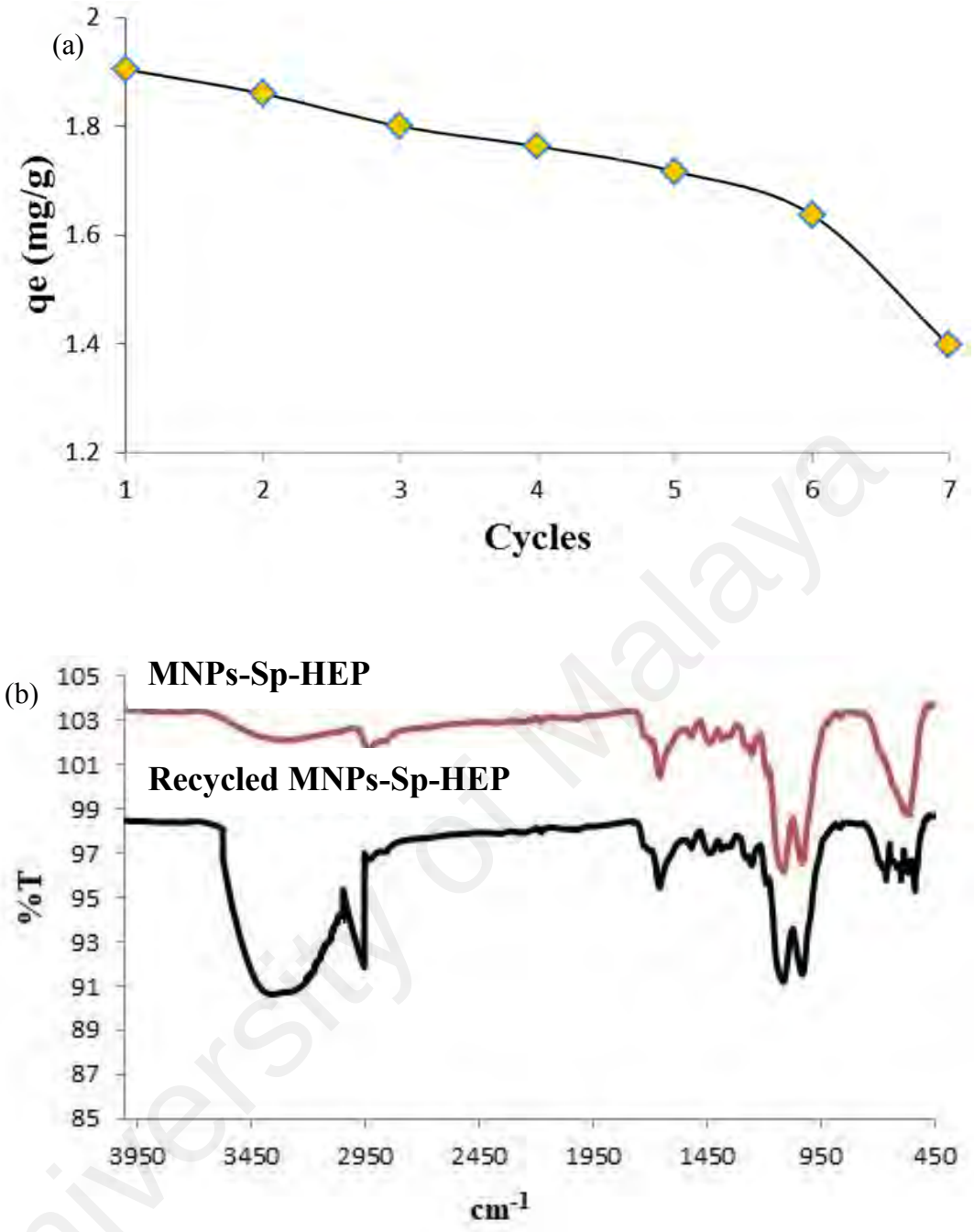

Figure 4.16 (a) Seven adsorption– regeneration cycles of Pb(II) ions and (b) FT-IR spectrum of MNPs-Sp-HEP and recycled MNPs-Sp-HEP at 7 cycle

4.3.4 Evaluation of the proposed method

4.3.4.1 Analytical performances

In order to assess the validation of the proposed method, linearity, the limit of detection, the limit of quantification and repeatability were performed under optimum conditions. Analytical performance figures of merits are tabulated in Table 4.6.

Calibration curves obtained for the studied Pb(II) ions was linear over the range of 0.01-0.1 mg L^{-1} with R^2 is 0.9999. The LOD of this method is 0.005 mg L^{-1} indicating the suitability of this method as an efficient Pb(II) ions extractor as the LOD is low enough to satisfy the permissible threshold established by the Ministry of Health Malaysia which is 0.05 mg L^{-1} and 0.01 mg L^{-1} in the recommended raw water quality and drinking water quality standard respectively.

Table 4.6 Method validation data for (MSPE) of Pb(II) ions with MNPs-Sp-HEP

Analytical Parameter	Value
R^2	0.9999
Linear range (mg L^{-1})	0.01-0.1
LOD (mg L^{-1})	0.005
LOQ (mg L^{-1})	0.017
RSD (%) Inter-day, n=3	3.3
RSD (%) Intra-day, n=7	4.1
Recovery	96%

Repeatability studies were conducted for inter-day (three consecutive replicates for three days) and intra-day (seven consecutive replicates on the same day). The results were expressed as relative standard deviation (RSD %). This method demonstrated good precision, since the RSD (%) values were in the range of 3 - 5% (Zhang *et al*., 2010).

Comparative studies on the analytical performance of the proposed method with other developed methods are shown in Table 4.7. Obviously, the extraction of Pb(II) ions using MNPs-Sp-HEP provides sensitivity and high pre-concentration factor.

Table 4.7 Comparison of LODs and pre-concentration factor (PF) values of several sorbents reported in the literature for extraction of Pb(II) ions.

Sorbent	LOD (mg L^{-1})	PF	Reference
mGO/SiO2@coPPy-Th	0.65	36	(Molaei *et al*., 2017)
MGO-DVB-VA	2.4	40	(Khan *et al*., 2016)
M-PhCP	2.7	80	(Yilmaz et al., 2015)
Magnetic allylamine modified graphene oxide-poly(vinyl-acetate-co-divinylbenzene)	2.39	40	(Khan *et al*., 2016)
Sp-HEP-Fe_3O_4	0.005	47	This study

4.3.4.2 Applications of Sp-HEP-Fe_3O_4 in environmental samples

The proposed method was applied to clean and complex matrix taken from a river (clean matrix), a tap (clean matrix) and leachate (complex matrix) for the determination of Pb(II) ions metal ions using optimum conditions of MSPE, 140 mL sample volume, sample pH at 6.5, 15 minutes adsorption time, 3 mL 0.1 M HNO_3 as desorption solvent and 15 mg adsorbent. From the analysis of real samples, Pb(II) ions cannot be detected in all environmental samples (river water, tap water and leachate). The results indicated that the proposed method provides good recoveries 97% and 96% for tap water and river water respectively. However, leachate showed a slightly low recovery (87%) as compared to other water samples due to matrix effects. Thus, this method was effective and can be applied as a reliable MSPE method for the determination of lead ion in environmental samples.

Table 4.8 The recoveries and RSD of Pb(II) ions in real environmental water samples with spike concentration

Samples	20		40		60	
	Spiked ($\mu g\ L^{-1}$)					
	Found	Recovery (±RSD)	Found	Recovery (±RSD)	Found	Recovery (±RSD)
River water	19.3	93.6 (±2.0)	37.0	91.0 (±3.1)	54.7	90.5 (±2.2)
Tap water	18.5	96.2 (±1.5)	34.6	92.6 (±1.1)	55.8	94.8 (±1.7)
Leachate	15.5	87.0 (±4.1)	38.3	89.1 (±4.7)	37.0	90.1 (±4.2)

CHAPTER 5: CONCLUSION

5.1 Conclusion

Modification of Sp with HEP and its magnetization with iron oxide nanoparticle was successful. The synthesized nanocomposite was characterized by FTIR, XRD, and VSM. From the FT-IR results, the presence of functional groups (cyano group, siloxane group and nanoparticles group) of the modified Sp was found in the spectra indicated that the functionalization has taken place. X-ray diffraction shows the presence of amorphous materials which is Sp. Magnetization saturation analyses by VSM showed that MNPs-Sp-HEP has sufficient magnetization saturation for magnetic separation with a conventional magnet. The morphology and elemental composition of MNPs-Sp-HEP were further confirmed with field emission scanning electron microscope (FESEM) and energy dispersive spectroscopy (EDS) respectively.

The adsorption process of Pb(II) ions onto MNPs-Sp-HEP was shown to be pH dependent, with the optimum removal being observed at pH 6.5. Kinetics analysis indicated that the kinetic data is well- fitted in the pseudo second –order equation model. Thermodynamic studies revealed that the adsorption process was exothermic and the organization of adsorbate at the solid interface become more random as ion replacement reaction occurred. The equilibrium isotherm data fitted well into the Langmuir isotherm with the R^2 is 0.9734.

The optimized conditions of MNPs-Sp-HEP for MSPE were carefully selected as follows; sample at pH 6.5, 15 min extraction time, 0.3 mol L^{-1} HNO_3 as the elution solvent, 3 mL elution solvent volume, 10 min desorption time, 25 mg adsorbent dosage and 140 mL sample volume. The stability and reusability studies suggested that the MNPs-Sp-HEP could be used up to five cycles without significantly impacting its extraction capacity. It has good linearity in the range of 0.01 – 0.1 mg L^{-1} and limit of

detection at 0.005 mg L^{-1}. The application of MNPs-Sp-HEP as the MSPE sorbent was successfully performed by the analysis of Pb(II) ions in real samples; river water, tap water, and leachate.

REFERENCES

Aboul- Enein, H. (2003). *Separation Techniques in Clinical Chemistry* (p. 19). New York: Marcel Dekker Inc.

Adal, A., & Tarabar, A. (2016). Heavy Metal Toxicity: Background, Pathophysiology, *Epidemiology*. *Emedicine.medscape.com*. Retrieved 21 December 2016, from http:// emedicine.medscape.com/article.

Aguado, J., Arsuaga, J., Arencibia, A., Lindo, M., & Gascón, V. (2009). Aqueous heavy metals removal by adsorption on amine-functionalized mesoporous silica. *Journal of Hazardous Materials*, *163*(1), 213-221.

Aguilar-Arteaga, K., Rodriguez, J., & Barrado, E. (2010). Magnetic solids in analytical chemistry: A review. *Analytica Chimica Acta*, *674*(2), 157-165.

Ali, A., Hira Zafar, M. Z., ul Haq, I., Phull, A. R., Ali, J. S., & Hussain, A. (2016). Synthesis, characterization, applications, and challenges of iron oxide nanoparticles. *Nanotechnology, Science and Applications*, *9*, 49.

AlOthman, Z. A., Habila, M. A., Al-Shalan, N. H., Alfadul, S. M., Ali, R., Al alm Rashed, I. G., & Alfarhan, B. (2016). Adsorptive removal of Cu(II) and Pb(II) onto mixed-waste activated carbon: kinetic, thermodynamic, and competitive studies and application to real wastewater samples. *Arabian Journal of Geosciences*, *9*(4), 315.

Ambashta R.D., & Sillanpää M. (2010). Water purification using magnetic assistance: a review.
Journal of Hazardous Materials, 180(1), 38-49.

Ariizumi, T. and Toriyama, K., (2011) Genetic Regulation of Sporopollenin Synthesis and Pollen Exine Development, *Annual Review Plant Biology 62*, 437–460.

Arora, V., Sood, A., Shah, J., Kotnala, R. K., & Jain, T. K. (2016). Synthesis and characterization of thiolated pectin stabilized gold coated magnetic nanoparticles. *Materials Chemistry and Physics*, *173*, 161-167.

Baharin, S. N. A., Sarih, N. M., Mohamad, S., Shahabuddin, S., Sulaiman, K., & Ma'amor, A. (2016). Removal of endocrine disruptor di-(2-ethylhexyl) phthalate by modified polythiophene-coated magnetic nanoparticles: characterization, adsorption isotherm, kinetic study, thermodynamics. *RSC Advances*, *6*(50), 44655-44667.

Bakhshaei, S., Kamboh, M. A., Nodeh, H. R., Zain, S. M., Rozi, S. K. M., Mohamad, S., & Mohialdeen, I. A. M. (2016). Magnetic solid phase extraction of polycyclic aromatic hydrocarbons and chlorophenols based on cyano-ionic liquid functionalized magnetic nanoparticles and their determination by HPLC-DAD. *RSC Advances*, *6*(80), 77047-77058.

Begum, M., & Huq, S. I. (2016). Heavy metal contents in soils affected by industrial activities in a southern district of Bangladesh. *Bangladesh Journal of Scientific Research*, *29*(1), 11-17.

Binks, B. P., Boa, A. N., Kibble, M. A., Mackenzie, G., & Rocher, A. (2011). Sporopollenin capsules at fluid interfaces: particle-stabilised emulsions and liquid marbles. *Soft Matter*, *7*(8), 4017-4024.

Boyer C., Whittaker M.R., Bulmus V., Liu J., & Davis. (2010). The design and utility of polymer-stabilized iron-oxide nanoparticles for nanomedicine applications. *NPG Asia Materials*, *2*(1), 23-30.

Bridwell-Rabb, J., & Drennan, C. L. (2017). Vitamin B 12 in the spotlight again. *Current Opinion in Chemical Biology*, *37*, 63-70.

Brooks, J., & Shaw, G. (1972). Geochemistry of sporopollenin. *Chemical Geology*, *10*(1), 69-87.

Brosché, S., Denney, V., Weinberg, J., Calonzo, M. C., Withanage, H., & Clark, S. (2014). *Asia Regional Paint Report*. IPEN, *3*, 34.

Cheng Y., Yang C., He H., Zeng G., Zhao K., Yan Z. (2015) Biosorption of Pb(II) ions from aqueous solutions by waste biomass from biotrickling filters: kinetics, isotherms, and thermodynamics. *Journal Environmental Engineering*: *142*(9), 1–7.

Chen K. L, Mylon S. E, & Elimelech M. (2007). Enhanced aggregation of alginate-coated iron oxide (hematite) nanoparticles in the presence of calcium, strontium, and barium cations. *Langmuir*, *23*(11), 5920-5928.

Chiappe, C., Demontis, G., Di Bussolo, V., Rodriguez Douton, M., Rossella, F., & Pomelli, C. et al. (2017). From pollen grains to functionalized microcapsules: a facile chemical route using ionic liquids. *Green Chemistry*, *19*(4), 1028-1033.

Chou, W. L., Wang, C. T., Huang, K. Y., & Liu, T. C. (2011). Electrochemical removal of salicylic acid from aqueous solutions using aluminum electrodes. *Desalination*, *271*(1), 55-61.

Çimen, A., Bilgiç, A., Kursunlu, A., Gübbük, İ., & Uçan, H. (2014). Adsorptive removal of Co(II), Ni(II), and Cu(II) ions from aqueous media using chemically modified sporopollenin ofLycopodium clavatumas novel biosorbent. *Desalination And Water Treatment*, *52*(25-27), 4837-4847.

Clark, C. S., Rampal, K. G., Thuppil, V., Chen, C. K., Clark, R., & Roda, S. (2006). The lead content of currently available new residential paint in several Asian countries. *Environmental Research*, *102*(1), 9-12.

Clark, C., Rampal, K., Thuppil, V., Roda, S., Succop, P., & Menrath, W. et al. (2009). Lead levels in new enamel household paints from Asia, Africa and South America. *Environmental Research*, *109*(7), 930-936.

Daraei, H., Mittal, A., Noorisepehr, M., & Mittal, J. (2015). Separation of chromium from water samples using eggshell powder as a low-cost sorbent: Kinetic and thermodynamic studies. *Desalination and Water Treatment*, *53*(1), 214-220.

Diego-Taboada, A., Beckett, S. T., Atkin, S. L., & Mackenzie, G. (2014). Hollow pollen shells to enhance drug delivery. *Pharmaceutics*, *6*(1), 80-96.

Dias A. M, Hussain A., Marcos A. S., & Roque A. C.. (2011). A biotechnological perspective on the application of iron oxide magnetic colloids modified with polysaccharides. *Biotechnology Advances*, *29*(1), 142-155.

Dyab, A. K., Abdallah, E. M., Ahmed, S. A., & Rabee, M. M. (2016). Fabrication and Characterisation of Novel Natural Lycopodium clavatum Sporopollenin Microcapsules Loaded In-Situ with Nano-Magnetic Humic Acid-Metal Complexes. *Journal of Encapsulation and Adsorption Sciences*, *6*(04), 109.

El-Geundi, M. S., Nassar, M. M., Farrag, T. E., & Ahmed, M. H. (2012). Removal of an insecticide (methomyl) from aqueous solutions using natural clay. *Alexandria Engineering Journal*, *51*(1), 11-18.

Escudero, R., Espinoza, E. and Tovera F.J. (2013). Precipitation of Lead Species in a Pb-H_2O System. *Research Journal of Resent Sciences, 2*(9), 1-4.

Fadzil, F., Ibrahim, S., & Hanafiah, M. A. K. M. (2016). Adsorption of lead (II) onto organic acid modified rubber leaf powder: Batch and column studies. *Process Safety and Environmental Protection*, *100*, 1-8.

Farid, A., Lubna, A., Choo, T., Rahim, M., & Mazlin, M. (2016). A Review on the Chemical Pollution of Langat River, Malaysia. Asian Journal of Water, *Environment And Pollution*, *13*(1), 9-15.

Gao, Q., Luo, D., Ding, J., & Feng, Y. Q. (2010). Rapid magnetic solid-phase extraction based on magnetite/silica/poly (methacrylic acid–co–ethylene glycol dimethacrylate) composite microspheres for the determination of sulfonamide in milk samples. *Journal of Chromatography A*, *1217*(35), 5602-5609.

Georgiou, Y., Mouzourakis, E., Bourlinos, A., Zboril, R., Karakassides, M., & Douvalis, A. et al. (2016). Surface decoration of amine-rich carbon nitride with iron nanoparticles for arsenite (AsIII) uptake: The evolution of the Fe-phases under ambient conditions. *Journal of Hazardous Materials*, *312*, 243-253.

Girginova P. I., Daniel-da-Silva A. L., Lopes C. B., Figueira P., Otero M., Amaral V. S., Pereira E. & Trindade T. (2010). Silica coated magnetite particles for magnetic removal of Hg^{2+} from water. *Journal of Colloid and Interface Science, 345*(2), 234-240.

Gubbuk, I. H., Gürfidan, L., Erdemir, S., & Yilmaz, M. (2012). Surface modification of sporopollenin with calixarene derivative. *Water, Air, & Soil Pollution*, *223*(5), 2623-2632.

Gubbuk, I. H. (2011). Isotherms and thermodynamics for the sorption of heavy metal ions onto functionalized sporopollenin. *Journal of Hazardous Materials*, *186*(1), 416-422.

Gulson, B., Chiaradia, M., Davis, J., & O'Connor, G. (2016). Impact on the environment from steel bridge paint deterioration using lead isotopic tracing, paint compositions and soil deconstruction. *Science of the Total Environment*, *550*, 69-72.

Gupta A. K., & Gupta M. (2005). Synthesis and surface engineering of iron oxide nanoparticles for biomedical applications. *Biomaterials*, *26*(18), 3995-4021.

Gupta VK, Rastogi A (2008) Biosorption of lead from aqueous solutions by green algae spirogyra species: kinetics and equilibrium studies. *Journal of Hazardous Material 152*:407–414.

He, Z., Shentu, J., Yang, X., Baligar, V. C., Zhang, T., & Stoffella, P. J. (2015). Heavy metal contamination of soils: Sources, indicators and assessment. *Journal of Environmental Indicators*, *9*, 17-18.

He, Z. L., Yang, X. E., & Stoffella, P. J. (2005). Trace elements in agroecosystems and impacts on the environment. *Journal of Trace Elements in Medicine and Biology*, *19*(2), 125-140.

Ho, Y. S. (2006). Isotherms for the Sorption of Lead onto Peat: Comparison of Linear and Non-Linear Methods. *Polish Journal of Environmental Studies*, *15*(1).

Hola, K., Markova, Z., Zoppellaro, G., Tucek, J., & Zboril, R. (2015). Tailored functionalization of iron oxide nanoparticles for MRI, drug delivery, magnetic separation and immobilization of biosubstances. *Biotechnology Advances*, *33*(6), 1162-1176.

Ibrahim, H. M., & Khalid, N. (2007, December). Growing Shipping Traffic in the Strait of Malacca: Some Reflections on the Environmental Impact. *In Global Maritime and Intermodal Logistics Conference, Singapore*

Igwe, J. C., & Abia, A. A. (2007). Adsorption isotherm studies of Cd (II), Pb(II) and Zn (II) ions bioremediation from aqueous solution using unmodified and EDTA-modified maize cob. *Eclética Química*, *32*(1), 33-42.

Mohammad, A. (2014). *Green Chromatographic Technique: Separation and Purification of Organic and Inorganic Analytes* (p. 148). Dordrecht: Springer.

Jacobs, D. E., Clickner, R. P., Zhou, J. Y., Viet, S. M., Marker, D. A., Rogers, J. W., ... & Friedman, W. (2002). The prevalence of lead-based paint hazards in US housing. *Environmental Health Perspectives*, *110*(10), A599.

Jain, M., Garg, V., Kadirvelu, K., & Sillanpää, M. (2015). Adsorption of heavy metals from multi-metal aqueous solution by sunflower plant biomass-based carbons. *International Journal of Environmental Science And Technology*, *13*(2), 493-500.

Jaishankar, M., Tseten, T., Anbalagan, N., Mathew, B. B., & Beeregowda, K. N. (2014). Toxicity, mechanism and health effects of some heavy metals. *Interdisciplinary Toxicology*, *7*(2), 60-72.

Jalil, A. A., Triwahyono, S., Adam, S. H., Rahim, N. D., Aziz, M. A. A., Hairom, N. H. H., ... & Mohamadiah, M. K. A. (2010). Adsorption of methyl orange from aqueous solution onto calcined Lapindo volcanic mud. *Journal of Hazardous Materials*, *181*(1), 755-762.

Kabata-Pendias, A., & Pendias, H. (2001). *Trace elements in soils and plants* (3rd ed.). Boca Raton, Flor.: CRC Press.

Kader, M., Lamb, D. T., Mahbub, K. R., Megharaj, M., & Naidu, R. (2016). Predicting plant uptake and toxicity of lead (Pb) in long-term contaminated soils from derived transfer functions. *Environmental Science and Pollution Research*, *23*(15), 15460-15470.

Kamboh, M. A., Ibrahim, W. A. W., Nodeh, H. R., Sanagi, M. M., & Sherazi, S. T. H. (2016). The removal of organophosphorus pesticides from water using a new amino-substituted calixarene-based magnetic sporopollenin. *New Journal of Chemistry*, *40*(4), 3130-3138.

Kamboh, M. A., & Yilmaz, M. (2013). Synthesis of N-methylglucamine functionalized calix [4] arene based magnetic sporopollenin for the removal of boron from aqueous environment. *Desalination*, *310*, 67-74.

Kettley, S. J. (2001). *Novel derivatives of sporopollenin for potential applications in solid phase organic synthesis and drug delivery* (Doctoral dissertation, University of Hull).

Khan, M., Yilmaz, E., Sevinc, B., Sahmetlioglu, E., Shah, J., Jan, M. R., & Soylak, M. (2016). Preparation and characterization of magnetic allylamine modified graphene oxide-poly (vinyl acetate-co-divinylbenzene) nanocomposite for vortex assisted magnetic solid phase extraction of some metal ions. *Talanta*, *146*, 130-137.

Kumar, S., Nair, R. R., Pillai, P. B., Gupta, S. N., Iyengar, M. A. R., & Sood, A. K. (2014). Graphene oxide–$MnFe_2O_4$ magnetic nanohybrids for efficient removal of lead and arsenic from water. *ACS Applied Materials and Interfaces*, *6*(20), 17426-17436.

Lapwanit, S., Trakulsujaritchok, T., & Nongkhai, P. (2016). Chelating magnetic copolymer composite modified by click reaction for removal of heavy metal ions from aqueous solution. *Chemical Engineering Journal*, *289*, 286-295.

Landrigan, P. J. (2002). The worldwide problem of lead in petrol. *Bulletin of the World Health Organization*, *80*(10), 768-768.

Lin, Lee, & Chiu. (2005). Preparation and properties of poly(acrylic acid) oligomer stabilized superparamagnetic ferrofluid. *Journal of Colloid and Interface Science*, *291*(2), 411-420.

Liu, Q. S., Zheng, T., Wang, P., Jiang, J. P., & Li, N. (2010). Adsorption isotherm, kinetic and mechanism studies of some substituted phenols on activated carbon fibers. *Chemical Engineering Journal*, *157*(2), 348-356.

Liška, I. (2000). Fifty years of solid-phase extraction in water analysis – historical development and overview. *Journal of Chromatography A*, *885*(1-2), 3-16.

Mackenzie, G., Boa, A. N., Diego-Taboada, A., Atkin, S. L., & Sathyapalan, T. (2016). Sporopollenin, the least known yet toughest natural biopolymer. *Non-Polysaccharide Plant Polymeric Materials*, 6657.

Majewski P., & Thierry B. (2007). Functionalized magnetite nanoparticles—synthesis, properties, and bio applications. *Critical Reviews in Solid State and Materials Sciences*, *32*(3-4), 203-215.

Mahdavian A. R., & Mirrahimi M. A. S. (2010). Efficient separation of heavy metal cations by anchoring polyacrylic acid on superparamagnetic magnetite nanoparticles through surface modification. *Chemical Engineering Journal*, *159*(1), 264-271.

MeenaKumari, M., & Philip, D. (2015). Degradation of environment pollutant dyes using phytosynthesized metal nanocatalysts. *Spectrochimica Acta Part A: Molecular and Biomolecular Spectroscopy*, *135*, 632-638.

Mehdinia, A., Shoormeij, Z., & Jabbari, A. (2017). Trace determination of lead (II) ions by using a magnetic nanocomposite of the type Fe_3O_4/TiO_2/PPy as a sorbent, and FAAS for quantitation. *Microchimica Acta*, *184*(5), 1529-1537.

Molaei, K., Bagheri, H., Asgharinezhad, A. A., Ebrahimzadeh, H., & Shamsipur, M. (2017). SiO_2-coated magnetic graphene oxide modified with polypyrrole–polythiophene: A novel and efficient nanocomposite for solid phase extraction of trace amounts of heavy metals. *Talanta*, *167*, 607-616.

Moldoveany S., & David V. (2015). *Modern Sample Preparation for Chromatography*. Elsevier

Nair, D. G., Hansdah, K., Dhal, B., Mehta, K. D., & Pandey, B. D. (2012). Bioremoval of Chromium (Iii) from model tanning effluent by novel microbial isolate. *International Journal of Metallurgical Engineering*, *1*(2), 12-16.

Nielsen, F. H. (1990). New essential trace elements for the life sciences. *Biological Trace Element Research*, *26*(1), 599-611.

Nonkumwong J, Ananta S, Srisombat L (2016) Effective removal of lead(II) fromwastewater by amine-functionalizedmagnesium ferrite nanoparticles. *RSC Advances, 6*:47382–47393.

Orhan, I., Küpeli, E., Şener, B., & Yesilada, E. (2007). Appraisal of anti-inflammatory potential of the clubmoss, Lycopodium clavatum L. *Journal of Ethnopharmacology*, *109*(1), 146-150.

Tripathy, S. K., Banerjee, P. K., Suresh, N., Murthy, Y. R., & Singh, V. (2017). Dry High-Intensity Magnetic Separation In Mineral Industry—A Review Of Present Status And Future Prospects. *Mineral Processing and Extractive Metallurgy Review*, 1-27.

Pan B., Qiu H., Pan B., Nie G., Xiao L., Lv L., Zhang W., Zhng Q., Zheng S. (2010). Highly efficient removal of heavy metals by polymer-supported nanosized hydrated Fe (III) oxides: behavior and XPS study. *Water Research, 44*(3), 815-824.

Paunov, V. N., Mackenzie, G., & Stoyanov, S. D. (2007). Sporopollenin micro-reactors for in-situ preparation, encapsulation and targeted delivery of active components. *Journal of Materials Chemistry*, *17*(7), 609-612.

Rauh, V., & Margolis, A. (2016). Research Review: Environmental exposures, neurodevelopment, and child mental health - new paradigms for the study of brain and behavioral effects. *Journal of Child Psychology and Psychiatry*, 57(7), 775-793.

Rossi, E., Errea, M. I., de Cortalezzi, M. M. F., & Stripeikis, J. (2017). Selective determination of Cr (VI) by on-line solid phase extraction FI-SPE-FAAS using an ion exchanger resin as sorbent: An improvement treatment of the analytical signal. *Microchemical Journal*, *130*, 88-92.

Rozi, S. K. M., Nodeh, H. R., Kamboh, M. A., Manan, N. S. A., & Mohamad, S. (2017). Novel Palm Fatty Acid Functionalized Magnetite Nanoparticles for Magnetic Solid-Phase Extraction of Trace Polycyclic Aromatic Hydrocarbons from Environmental Samples. *Journal of Oleo Science*, *66*(7), 771-784.

Sáez, C., de Vidales, M. J. M., Cañizares, P., Cotillas, S., Llanos, J., Pérez, J. F., & Rodrigo, M. A. (2014). Irradiated electrochemical processes for the removal of persistent organic pollutants from waters and wastewaters. *Chemical Engineering Trans Actions*, *41*,103–108.

Sadeghi, M., Yekta, S., & Babanezhad, E. (2016). Immobilization of the Thenoyltrifluoroacetone on Sodium Dodecyl Sulfate Modified Magnetite Nanoparticles for Magnetic Solid Phase Extraction of Pb(II) from Water Samples. *Korean Chemical Engineering Research* (*화학공학*), *54*(5), 636-647.

Selwyn, L. (2005). Health and Safety Concerns Relating to Lead and Lead Compounds in Conservation. *Journal of The Canadian Association For Conservation*, *30*, 18-37.

Sears, M. E., Kerr, K. J., & Bray, R. I. (2012). Arsenic, cadmium, lead, and mercury in sweat: a systematic review. *Journal of Environmental and Public Health*, 2012.

Şener, M., Kayan, B., Akay, S., Gözmen, B., & Kalderis, D. (2016). Fe-modified sporopollenin as a composite biosorbent for the removal of Pb^{2+} from aqueous solutions. *Desalination and Water Treatment*, *57*(58), 28294-28312.

Şener, M., Reddy, D. H. K., & Kayan, B. (2014). Biosorption properties of pretreated sporopollenin biomass for lead (II) and copper (II): Application of response surface methodology. *Ecological Engineering*, *68*, 200-208.

Shahabuddin, S., Sarih, N. M., Afzal Kamboh, M., Rashidi Nodeh, H., & Mohamad, S. (2016). Synthesis of Polyaniline-Coated Graphene Oxide@ $SrTiO_3$ Nanocube Nanocomposites for Enhanced Removal of Carcinogenic Dyes from Aqueous Solution. *Polymers*, *8*(9), 305.

Shamsipur, M., Farzin, L., Tabrizi, M. A., & Sheibani, S. (2017). Functionalized Fe_3O_4/graphene oxide nanocomposites with hairpin aptamers for the separation and pre-concentration of trace Pb^{2+} from biological samples prior to determination by ICP MS. *Materials Science and Engineering: C*, *77*, 459-469.

Shazili, N. A. M., Yunus, K., Ahmad, A. S., Abdullah, N., & Rashid, M. K. A. (2006). Heavy metal pollution status in the Malaysian aquatic environment. *Aquatic Ecosystem Health and Management*, *9*(2), 137-145.

Shrivastava, A., & Gupta, V. (2011). Methods for the determination of limit of detection and limit of quantitation of the analytical methods. *Chronicles of Young Scientists*, *2*(1), 21-21.

Singh, A. K., & Singh, M. (2006). Lead decline in the Indian environment resulting from the petrol-lead phase-out programme. *Science of the Total Environment*, *368*(2), 686-694.

Sivashankar, R., Sathya, A. B., Vasantharaj, K., & Sivasubramanian, V. (2014). Magnetic composite an environmental super adsorbent for dye sequestration–A review. *Environmental Nanotechnology, Monitoring and Management*, *1*, 36-49.

Sureshkumar, V., Daniel, S. K., Ruckmani, K., & Sivakumar, M. (2016). Fabrication of chitosan–magnetite nanocomposite strip for chromium removal. *Applied Nanoscience*, *6*(2), 277-285.

Tahmasebi, E., Yamini, Y., Moradi, M., & Esrafili, A. (2013). Polythiophene-coated Fe_3O_4 superparamagnetic nanocomposite: synthesis and application as a new sorbent for solid-phase extraction. *Analytica Chimica Acta*, *770*, 68-74.

Tangahu, B. V., Sheikh Abdullah, S. R., Basri, H., Idris, M., Anuar, N., & Mukhlisin, M. (2011). A Review on heavy metals (As, Pb, and Hg) uptake by plants through phytoremediation. *International Journal of Chemical Engineering*, 2011.

Tchounwou, P. B., Yedjou, C. G., Patlolla, A. K., & Sutton, D. J. (2012). Heavy metal toxicity and the environment. In *Molecular, Clinical and Environmental Toxicology* (pp. 133-164). Springer Basel.

Thompson, K., & Orvig, C. (2003). Boon and Bane of Metal Ions in Medicine. *Science*, *300*(5621), 936-939.

Tutar, H., Yilmaz, E., Pehlivan, E. and Yilmaz, M. (2009). Immobilization of Candida rugose lipase on sporopollenin from Lycopodium clavatum. *International Journal of Biological Macromolecules, 45*(3), 315-320.

Uçar, S., Erdem, M., Tay, T., & Karagöz, S. (2014). Removal of lead (II) and nickel (II) ions from aqueous solution using activated carbon prepared from rapeseed oil cake by Na_2CO_3 activation. *Clean Technologies and Environmental Policy*, *17*(3), 747-756.

Ünlü, N., & Ersoz, M. (2006). Adsorption characteristics of heavy metal ions onto a low cost biopolymeric sorbent from aqueous solutions. *Journal of Hazardous Materials*, *136*(2), 272-280.

Vasconcelos, I., & Fernandes, C. (2017). Magnetic solid phase extraction for determination of drugs in biological matrices. *TrAC Trends in Analytical Chemistry*.

Vymazal, J., & Březinová, T. (2015). The use of constructed wetlands for removal of pesticides from agricultural runoff and drainage: a review. *Environment International*, *75*, 11-20.

Wan Ibrahim. W. A., Nodeh, H. R., & Sanagi, M. M. (2016). Graphene-based materials as solid phase extraction sorbent for trace metal ions, organic compounds, and biological sample preparation. *Critical Reviews in Analytical Chemistry*, *46*(4), 267-283.

Wan Ibrahim, W. A., Nodeh, H. R., Aboul-Enein, H. Y., & Sanagi, M. M. (2015). Magnetic solid-phase extraction based on modified ferum oxides for enrichment, pre-concentration, and isolation of pesticides and selected pollutants. *Critical Reviews in Analytical Chemistry*, *45*(3), 270-287.

Wan Ibrahim, W. A., Veloo, K. V. and Sanagi, M. M. (2012). Novel sol-gel hybrid methyltrimethoxysilane-tetraethoxysilane as solid phase extraction sorbent for organophosphorus pesticides. *Journal of Chromatography A*. *1229*, 55–62.

Wang, L. K., Chen, J. P., Hung, Y. T., & Shammas, N. K. (Eds.). (2009). *Heavy metals in the Environment*. CRC Press.

White B. R., Stackhouse B. T., & Holcombe J.A. (2009). Magnetic γ-Fe_2O_3 nanoparticles coated with poly-l-cysteine for chelation of As (III), Cu(II), Cd(II), Ni(II), Pb(II) and Zn (II). *Journal of Hazardous Materials, 161*(2), 848-853.

Woźniak, E., Špírková, M., Šlouf, M., Garamus, V., Šafaříková, M., Šafařík, I., & Štěpánek, M. (2017). Stabilization of aqueous dispersions of poly(methacrylic acid)-coated iron oxide nanoparticles by double hydrophilic block polyelectrolyte poly(ethylene oxide)- block -poly(N -methyl-2-vinylpyridinium iodide). *Colloids And Surfaces A: Physicochemical And Engineering Aspects*, *514*, 32-37.

Wu, W., He, Q., & Jiang, C. (2008). Magnetic iron oxide nanoparticles: synthesis and surface functionalization strategies. *Nanoscale Research Letters*, *3*(11), 397.

Wolfe, P. J., Giang, A., Ashok, A., Selin, N. E., & Barrett, S. R. (2016). Costs of IQ loss from leaded aviation gasoline emissions. *Environmental Science & technology*, *50*(17), 9026-9033.

Xie, Jiang, Zhu, Liu, & Ouyang. (2014). Application of functionalized magnetic nanoparticles in sample preparation. *Analytical and Bioanalytical Chemistry*, *406*(2), 377-399.

Yilmaz, E., Alosmanov, R., & Soylak, M. (2015). Magnetic solid phase extraction of lead(II) and cadmium(ii) on a magnetic phosphorus-containing polymer (M-PhCP) for their microsampling flame atomic absorption spectrometric determinations. *RSC Advances*, *5*(43), 33801-33808.

Zhang, C. (2007). *Fundamentals of Environmental Sampling and Analysis*. John Wiley & Sons.

Zhang, L. S., Jiang, L. Y., Yan, H. J., Wang, W. D., Wang, W., Song, W. G., ... & Wan, L. J. (2010). Mono dispersed SnO 2 nanoparticles on both sides of single layer graphene sheets as anode materials in Li-ion batteries. Journal of Materials Chemistry, 20(26), 5462-5467.

Zhang, M., Zhang, Z., Liu, Y., Yang, X., Luo, L., Chen, J., & Yao, S. (2011). Preparation of core–shell magnetic ion-imprinted polymer for selective extraction of Pb(II) from environmental samples. *Chemical Engineering Journal*, *178*, 443-450.

Zheng, X., He, L., Duan, Y., Jiang, X., Xiang, G., Zhao, W., & Zhang, S. (2014). Poly (ionic liquid) immobilized magnetic nanoparticles as new adsorbent for extraction and enrichment of organophosphorus pesticides from tea drinks. *Journal of Chromatography A*, *1358*, 39-45.

LIST OF PUBLICATION AND PAPER PRESENTED

Publication:

Ahmad, N. F., Kamboh, M. A., Nodeh, H. R., Halim, S. N. B. A., & Mohamad, S. (2017). Synthesis of piperazine functionalized magnetic sporopollenin: a new organic-inorganic hybrid material for the removal of lead (II) and arsenic (III) from aqueous solution. *Environmental Science and Pollution Research*, 24(27), 21846–21858.

Proceeding/ presentation:

Ahmad, N. F., Kamboh, M. A., Nodeh, H. R., Halim, S. N. B. A., & Mohamad, S. (2017). Synthesis of piperazine functionalized magnetic sporopollenin: a new organic-inorganic hybrid material for the removal of lead (II) and arsenic (III) from aqueous solution, The 29th Malaysian Analytical Chemistry Symposium, (2016), Penang, Malaysia.